UNCLASSIFIED

AD NUMBER: AD0868895

LIMITATION CHANGES

TO:

Approved for public release; distribution is unlimited.

FROM:

Distribution authorized to US Government Agencies Only; Export Control; 1 Dec 1969. Other requests shall be referred to US Army Missile Command, Redstone Arsenal, AL 35809.

AUTHORITY

USAMICOM ltr dtd 7 Dec 1972

THIS PAGE IS UNCLASSIFIED

AD 868895

AD

REPORT NO. RD-TR-69-13

ANALYSIS OF THE AXISYMMETRIC BASE-PRESSURE AND BASE-TEMPERATURE PROBLEM WITH SUPERSONIC INTERACTING FREESTREAM-NOZZLE FLOWS BASED ON THE FLOW MODEL OF KORST, ET AL.

PART II: A COMPARISON AND CORRELATION WITH EXPERIMENT FOR CYLINDRICAL AFTERBODIES

by

A. L. Addy

December 1969

This document is subject to special export controls and each transmittal to foreign governments or foreign nationals may be made only with prior approval of this Command, ATTN: AMSMI-RD.

U.S. ARMY MISSILE COMMAND
Redstone Arsenal, Alabama 35809

DDC
RECEIVED
MAY 11 1970
C

67

ACCESSION for
NTIS WHITE SECTION
DDC BUFF SECTION
UNANNOUNCED
JUSTIFICATION
BY
DISTRIBUTION/AVAILABILITY CODES
DIST. AVAIL. and/or SPECIAL
2

DISPOSITION INSTRUCTIONS

Destroy this report when it is no longer needed. Do not return it to the originator.

TRADE NAMES

Use of trade names or manufacturers in this report does not constitute an official endorsement or approval of the use of such commercial hardware or software.

DISCLAIMER

The findings in this report are not to be construed as an official Department of the Army position unless so designated by other authorized documents.

BLANK PAGE

December 1969 Report No. RD-TR-69-13

ANALYSIS OF THE AXISYMMETRIC BASE-PRESSURE AND BASE-TEMPERATURE PROBLEM WITH SUPERSONIC INTERACTING FREESTREAM-NOZZLE FLOWS BASED ON THE FLOW MODEL OF KORST, ET AL.

PART II: A COMPARISON AND CORRELATION WITH EXPERIMENT FOR CYLINDRICAL AFTERBODIES

by

A. L. ADDY†

AMC MANAGEMENT STRUCTURE CODE NO. 522A.11.14800

DA PROJECT NO. 1M62301A206

This document is subject to special export controls and each transmittal to foreign governments or foreign nationals may be made only with prior approval of this Command, ATTN: AMSMI-RDK

Aerodynamics Branch
Advanced Systems Laboratory
Research and Engineering Directorate
U.S. Army Missile Command
Redstone Arsenal, Alabama 35809

---

†Associate Professor of Mechanical Engineering, University of Illinois at Urbana-Champaign; Consultant, Army Research Office-Durham.

ABSTRACT

The functional behavior and the effects of the many geometric and flow variables on the base-pressure and base-temperature ratios can be qualitat vely predicted with the flow model of Korst, et al. Although he predicted trends are correct, the discrepancy between predicted and experimental values of the base-pressure ratios can be significant under certain conditions of geometry and flow. To improve predicted-experimental agreement and to establish a basis for a quantitative analysis of the base-pressure problem with this flow model, a modification to the flow model based on an empirically determined recompression coefficient is proposed. The recompression coefficient and its principal dependence on the nozzle-to-base radius ratio are established by detailed comparisons with experiment over a wide range of the governing variables. The recompression coefficient and the detailed comparisons with experimental data are presented herein.

TABLE OF CONTENTS

		Page
	LIST OF FIGURES	iv
	LIST OF TABLES	vi
	NOMENCLATURE	vii
I.	INTRODUCTION	1
II.	EMPIRICAL FLOW-MODEL MODIFICATION	4
	A. RECOMPRESSION COEFFICIENT DEFINITION	4
	B. RECOMPRESSION COEFFICIENT DETERMINATION	5
III.	DETAILED COMPARISONS WITH EXPERIMENT	7
IV.	CONCLUSIONS	8
	REFERENCES	9
	FIGURES AND TABLES	12

LIST OF FIGURES

Page

Figure 1. Two-Stream Axisymmetric Base-Flow Configuration and Notation 20

Figure 2. Definition of the Empirical Recompression Coefficient 21

Figure 3. Functional Behavior of the Recompression Coefficient 22

Figure 4. A Comparison with the Data of Cortright and Schroeder [8] 23

Figure 5. A Comparison with the Data of Messing, et al. [9] . . . 24

Figure 6. A Comparison with the Data of Bromm, et al. [10]
(a) Variations in $\bar{R}_{1I}$ and M_{1E} 25
(b) Variations in β_{1I} ($M_{1I} = 3$, $M_{1E} = 1.62$, $\bar{R}_{1I} = 0.75$) 26
(c) Variations in β_{1I} ($M_{1I} = 3$, $M_{1E} = 1.94$, $\bar{R}_{1I} = 0.75$) 27

Figure 7. A Comparison with the Data of Baughman and Kochendorfer [11] 28

Figure 8. A Comparison with the Data of Reid and Hastings [12] . 29

Figure 9. A Comparison with the Data of Henderson [13]
(a) Variations in $\bar{R}_{1I}$ ($M_{1E} = 1.65$, $\beta_{1I} = 15°$) 30
(b) Variations in $\bar{R}_{1I}$ ($M_{1E} = 1.82$, $\beta_{1I} = 0°$) 31
(c) Variations in $\bar{R}_{1I}$ ($M_{1E} = 1.82$, $\beta_{1I} = 15°$) 32
(d) Variations in $\bar{R}_{1I}$ ($M_{1E} = 2.21$, $\beta_{1I} = 0°$) 33
(e) Variations in $\bar{R}_{1I}$ ($M_{1E} = 2.21$, $\beta_{1I} = 15°$) 34

Figure 10. A Comparison with the Data of Craven, et al. [14] . . . 35

Figure 11. A Comparison with the Data of Charczenko and Hayes [15] 36

Figure 12. A Comparison with the Data of Roberts and Golesworthy [16] 37

Figure 13. A Comparison with the Data of White [17] 38

Figure 14. A Comparison with the Data of Harries [18]
(a) Variations in M_{1E} 39
(b) Variation in P_{1I}/P_{1E} 40

Figure 15. A Comparison with the Data of Reid [19]
(a) Variation in T_{oI}/T_{oE} for given Values of P_{oI}/P_E ($\bar{R}_{II} = 0.5$) 41
(b) Variation in T_{oI}/T_{oE} for given Values of P_{oI}/P_E ($\bar{R}_{II} = 0.645$) 42

Figure 16. A Comparison with the Data of Brazzel [20]
(a) Variations in $\bar{R}_{II}$ ($M_{1E} = 2.5$, $M_{1I} = 1.0$) 43
(b) Variations in $\bar{R}_{II}$ ($M_{1E} = 2.5$, $M_{1I} = 1.78$, $\beta_{II} = 20°$) 44
(c) Variations in $\bar{R}_{II}$ ($M_{1E} = 2.5$, $M_{1I} = 2.7$, $\beta_{II} = 20°$) 45
(d) Large-range Variation in P_{oI}/P_{1E} ($M_{1E} = 2.5$, $M_{1I} = 2.7$, $\beta_{II} = 20°$) 46
(e) Variations in $\bar{R}_{II}$ ($M_{1E} = 3.0$, $M_{1I} = 1.0$, $\beta_{II} = 0°$) 47
(f) Variations in $\bar{R}_{II}$ ($M_{1E} = 3.0$, $M_{1I} = 1.78$, $\beta_{II} = 20°$) 48
(g) Variations in $\bar{R}_{II}$ ($M_{1E} = 3.0$, $M_{1I} = 2.7$, $\beta_{II} = 20°$) 49
(h) Variations in M_{1E} ($M_{1I} = 1.0$, $\bar{R}_{II} = 0.45$) 50
(i) Variations in β_{II} ($M_{1E} = 1.5$, $M_{1I} = 2.7$, $R_{II} = 0.8$) 51
(j) Variations in β_{II} ($M_{1E} = 2.5$, $M_{1I} = 2.7$, $R_{II} = 0.8$) 52
(k) Large-range Variations in P_{oI}/P_{1E} ($M_{1E} = 2.5$, $M_{1I} = 3.8$, $\beta_{II} = 20°$, $\bar{R}_{II} = 0.8$) 53

Figure 17. A Limited Comparison with the Data Obtained at the University of Illinois at Urbana-Champaign [21]
(a) Variations in M_{1I} 54
(b) Variations in γ_I 55

LIST OF TABLES

Page

Table I A Tabulation of Data Sources and Ranges of Variables Used in the Determination of the Recompression Coefficient 12

NOMENCLATURE†

I. SYMBOLS

C	Crocco number, (U/U_{max})
E_o	Energy transfer rate into the base region
E_{NI}	Energy transfer rate based on the total enthalpy of an ideal propulsive nozzle (reference value)
$f(\ )$	Functional notation
G_o	The "bleed" mass flow rate into the base region
G_{NI}	Mass flow rate of an ideal propulsive nozzle (reference value)
M	Mach number
P	Absolute pressure
r	Empirical recompression coefficient
R	Radius
$\mathbb{R}$	Gas constant
T	Absolute temperature
X,R	Longitudinal and radial coordinate, respectively
β	Flow angle
γ	Ratio of specific heats
δ^*,δ^{**}	Boundary layer displacement and momentum thickness, respectively

†See NOMENCLATURE of Part I, [2], for supplemental definitions.

II. SUBSCRIPTS

B	Base region
d	Discriminating streamline
E	External (freestream) flow
I	Internal (nozzle) flow
oE, oI	Stagnation condition for external and internal flow, respectively
S	Slipline; conditions immediately downstream of the oblique-shock recompression system
1E, 1I	Separation point for the external and internal stream, respectively

III. BARRED SYMBOLS (Dimensionless Ratios)

$\overline{B}_o$	Dimensionless mass "bleed" rate, G_o/G_{NI}
$\overline{E}_o$	Dimensionless energy transfer rate, E_o/E_{NI}
$\overline{P}_B$	Base-Pressure ratio, P_B/P_{1E}
$\overline{P}_{1I}$	Nozzle exit plane-to-freestream static pressure ratio, P_{1I}/P_{1E}
$\overline{P}_{oI}$	Internal stagnation-to-external static pressure ratio, P_{oI}/P_{1E}
$\overline{R}_I$	Ratio of gas constants, R_I/R_E
$\overline{T}_B$	Base-temperature ratio, T_B/T_{oI}
$\overline{T}_{oE}$	External-to-internal stream stagnation temperature ratio, T_{oE}/T_{oI}
$\overline{X}_{1I}$, $\overline{R}_{1I}$	Dimensionless coordinate of the separation point of the internal stream: X_{1I}/R_{1E}, R_{1I}/R_{1E}

BLANK PAGE

I. INTRODUCTION

Base drag constitutes a significant part of the overall vehicle drag under powered supersonic flight conditions; as a consequence, proper evaluation of the base-drag contribution is essential for meaningful evaluation, design, or optimization studies. The component flow model of Korst, et al. [1,2]† is well-suited for these studies, since it offers a tenable method for predicting the influence and relative significance of the many flow and geometrical variables involved. In addition, the component aspects of this flow model are readily adaptable to computerized analyses, e.g., as presented as Part I of this report [2].

Experience has shown that general trends and the functional dependence of base-pressure and base-temperature ratios on the governing variables can be predicted correctly with this flow model. There are, however, geometrical and flow conditions wherein significant discrepancies exist between the level of predicted and experimental values of the base-pressure ratio; these discrepancies are most pronounced for those cases wherein the nozzle is relatively small in comparison with the base.

Some reasons for the observed discrepancies between predicted and experimental values have long been recognized by the investigators associated with the original development and the subsequent application of this flow model, as well as with the parent two-dimensional Chapman-Korst flow model. For this study, these discrepancies could be attributed, not necessarily in their order of importance, to:

i. The approximation of an axisymmetric mixing region by the superposition of a plane two-dimensional mixing region.

ii. The non-constant pressure nature of the base region resulting from the mutual interaction among the entrained flows, the recirculating flows, and the nearly-inviscid supersonic streams.

iii. The influence of the boundary layers which modify the mixing regions, the centered expansions, and the "apparent" mass addition to the base region.

iv. The recompression criterion which distinguishes between the "escaping" and "recirculating" flows, and as such, establishes a basis for determining the base-flow solution.

---

†Numbers in brackets refer to entries in REFERENCES.

The recompression process is central in determining the base-flow solution since it links the components of the flow model: The "corresponding" inviscid flowfield and turbulent mixing components. Since the recompression process is not well understood and does strongly influence the solution to the base-flow problem, the need to improve agreement between predicted and experimental values has resulted in several empirical modifications to this part of the flow model.

Nash [3] proposed and determined an empirical "reattachment condition" for the supersonic single-stream two-dimensional case which was approximately independent of the supersonic approach Mach number. An approach was adopted by Carriere and Sirieix [4] in which they proposed and meticulously determined an empirical law of reattachment, for a negligible initial boundary layer, based on an "angular criterion of turbulent reattachment." Their proposed law of reattachment is shown to correlate well the data for reattachment at a wall of supersonic axisymmetric, two-dimensional, and conical flows. Page, Kessler, and Hill [5] offer an alternative empirical reattachment for two-dimensional supersonic flows based on the "discriminating-streamline" velocity ratio.

For the axisymmetric two-stream base-flow problem under consideration herein, the recompression resulting from the interaction of separated supersonic freestream-nozzle flows apparently cannot be analyzed by a direct carry-over of the empirical reattachment criteria determined in the aforementioned investigations. As a result, Sirieix, Délery, and Mirande [6] have presented a more generalized "criterion of turbulent reattachment" which involves geometric, as well as flow variables. This criterion is the basis for a limited comparison between predicted and experimental values of the axisymmetric jet-on base-pressure ratio. Agreement was improved for the cases presented. More recently, Dixon, Richardson, and Page [7] considered this problem under the experimentally supported assumption that the external inviscid flow boundary remains straight after initially turning to adjust to the base pressure. This assumption necessarily results in an axial-pressure gradient from which the internal flow boundary is determined. The "corresponding" inviscid flowfields thus determined are linked to an approximate axisymmetric mixing component by a recompression criterion based on Goethert's modification of Korst's "escape criterion." This approach also improves the agreement between the predicted and experimental results for the cases presented in their paper.

With this background and the availability of a computer program based on the flow model of Korst, et al. [2], a somewhat simpler empirical flow-model modification than the foregoing is proposed herein. The recompression criterion is modified by assuming that the discriminating streamlines or the jet-boundary streamlines, as

the case may be, are capable of recompressing by stagnating only to a fraction of the pressure rise from the base region to the downstream shock region as determined for the "corresponding" inviscid flowfields. The unknown fractional pressure rise must be determined from experiment and, in general, would be expected to be a function of the many governing dimensionless groups associated with this problem. However, detailed comparisons with approximately one hundred and fifty sets of experimental data have shown that the recompression coefficient, so defined, is principally a function of one dimensionless geometrical variable: The nozzle-to-base radius ratio. Although data used in these comparisons represented a wide range of geometrical and flow variables, they were obtained principally in cold flow air-to-air experiments. With a single value of this empirical coefficient which corresponds to a particular geometrical configuration good agreement can be achieved throughout the range of variation in the usual independent variable: The internal-to-external streams pressure ratio.

The definition and functional behavior of the proposed empirical recompression coefficient are presented in the following sections; in addition, many of the predicted-experimental comparisons used in determining this empirical-correlation coefficient are also presented.

II. EMPIRICAL FLOW-MODEL MODIFICATION

The configuration and the associated notation for the present study of the supersonic axisymmetric base-flow problem with nozzle flow and a cylindrical afterbody is shown in Fig. 1. Internal and external streams are assumed to separate at locations (1I) and (1E), respectively, and as a consequence, the resulting separated supersonic streams subsequently interact, forming a shock recompression system at the impingement point of the streams.

The flow model separates the analysis into the mixing component, "corresponding" inviscid flowfields, and the linking of mixing-inviscid components by the recompression criterion. Recompression pressure rise is associated with the oblique shock system resulting from the impingement of "corresponding" inviscid supersonic streams; this pressure rise is the basis for distinguishing between the fluid energized by the mixing which has sufficient mechanical energy to recompress to this pressure level from that which has insufficient mechanical energy and, as a consequence, must recirculate into the base region. The base-flow solution is then determined by the requirement of conservation of mass and energy for the overall base region.

The recompression coefficient modification to the flow model consists, essentially, of redefining the level of pressure to which discriminating streamlines (d-streamlines) must recompress.

A. RECOMPRESSION COEFFICIENT DEFINITION

If the pressure rise immediately downstream of the oblique shock system, Fig. 2, is given relative to the base pressure as (P_S/P_B), then the pressure level to which the discriminating streamline must recompress by stagnating is assumed to be given by, [2, pp. 4-10],

$$\frac{P_{od}}{P_d}(C_d,\gamma) = r\left(\frac{P_S}{P_B}\right) > 1 \qquad (1)$$

Equation (1) serves as the definition for the yet-to-be-determined empirical recompression coefficient r. At the outset, it is reasonable to assume that r could be a function of the numerous dimensionless groups governing this problem. In general, the functional form of r could be expressed as

$$r = f(\bar{X}_{11}, \bar{R}_{11}, \beta_{11}, M_{11}, \gamma_1, \bar{R}_1, M_{1E}, \gamma_E, \bar{T}_{oE}, \bar{B}_o, \bar{E}_o, \bar{P}_{11}, \bar{\delta}^*_{11}, \bar{\delta}^{**}_{11}, \bar{\delta}^*_{1E}, \bar{\delta}^{**}_{1E}) \quad (2)$$

If r were indeed strongly dependent on all the above dimensionless variables, the possibility of determining its functional form would, of course, be remote. However, since the flow model considers and apparently adequately accounts for many of the variables in the inviscid, viscid, or recompression components of the flow model, the influence on r of some of the variables would be expected to be small. This indeed has been found to be the case.

B. RECOMPRESSION COEFFICIENT DETERMINATION

Determination of the form of Eq. (2) then must be based on a detailed comparison between predicted and experimental data. Most of the experimental data reported in the literature and determined in connection with the continuing study of the base-flow problem, [8-21], have been obtained principally in small scale, cold-flow, air-to-air model studies. Generally, the experimental programs and available data can be classed according to the grouping of and variation in the variables of Eq. (2).

Many of the available experimental data have been obtained in studies wherein variations were made principally in the following variables:

$$[\bar{R}_{11}, \beta_{11}, M_{11}, M_{1E}, \bar{B}_o, \bar{P}_{11}]$$

Data for the more difficult experimental studies dealing with variations in the variables

$$[\gamma_1, \bar{R}_1, \bar{T}_{oE}]$$

are limited in quantity and scope. An assessment of the influence of boundary layers, which are characterized by values of

$$[\bar{\delta}^*_{11}, \bar{\delta}^{**}_{11}, \bar{\delta}^*_{1E}, \bar{\delta}^{**}_{1E}]$$

is complicated by the lack of complete data on the boundary layers

or by the small scale of the model wherein boundary layer effects are small or have been reduced intentionally. As a consequence, only a qualitative indication of the causal relationship between the base-pressure ratio and the boundary layers can be inferred.

The sources and the variation(s) in the variable(s) for experimental data used in the determination of the recompression coefficient are tabulated in Table I. Values of r were determined by comparing experimental data with predicted values for a given configuration. The procedure followed was to start the comparison for the unmodified model (r = 1) and then systematically vary r until a value of r was determined which would give reasonably "good" agreement between predicted and experimental data throughout the range of the principal independent variable. In most cases, the independent variable was the nozzle-to-freestream pressure ratio.

Values of the recompression coefficient thus determined for the cases tabulated in Table I, are presented in Fig. 3 as a function of the nozzle-to-base radius ratio, $\bar{R}_{11}$. Values of the recompression coefficient are seen from Fig. 3 to be influenced most strongly by $\bar{R}_{11}$ in comparison with all other variables. In cases wherein adequate experimental data were available, it was possible to determine the maximum variation in r for a given value of $\bar{R}_{11}$; these variations are indicated in Fig. 3. Some variation in values of r can be attributed to the dependence, although small, of the recompression coefficient on the other variables, as well as the boundary layers, which have been neglected in this study.

Based on values of the recompression coefficient presented in Fig. 3, a convenient least-squares representation of the recompression coefficient is given by

$$r = 0.483 + 1.088\,\bar{R}_{11} - 0.874\,\bar{R}_{11}^2 + 0.303\,\bar{R}_{11}^3 \qquad (3)$$

The standard error for this curve fit is $s_r = 0.0151$. Equation (3) is also plotted in Fig. 3.

III. DETAILED COMPARISONS WITH EXPERIMENT

The comparisons between experimental and predicted values which were used in determining appropriate values of the recompression coefficient are presented in Figs. 4-17. For each case or set of experimental data, geometric and flow variables are specified completely and related to the appropriate figure for comparison in Table I.

The objectives in presenting the detailed comparisons are two-fold: First, to compile and present experimental data with significant variations in the flow and configuration variables and secondly, to demonstrate the degree of correlation that can be achieved between experimental and predicted values when the recompression coefficient is utilized. Again, comparisons with the data of references [8-21] are presented in Figs. 4-17.

IV. CONCLUSIONS

Modification of the flow model of Korst, et al., by an empirically determined recompression appears to be justified adequately, based on the detailed comparisons presented. As a consequence, quantitative analyses for evaluation, design, and optimization studies can be made with a degree of confidence in the results by using the recompression coefficient in conjunction with the available computer program [2]. Also, the recompression coefficient provides a basis for a unified comparison between the diversity of available experimental data.

The general behavior of the recompression coefficient illustrates that as the nozzle-to-base radius ratio approaches unity, the axisymmetric nature is decreased and, as such, more nearly approximates the plane two-dimensional case. On the other hand, as the radius ratio is decreased, the axisymmetric nature of the problem is more and more strongly reflected in the somewhat unrealistic nature of the inviscid external-flow boundary; thus, the values of the recompression coefficient must necessarily decrease from unity--the basic flow model.

The influence of boundary layers, particularly for the external stream, should be considered. Many of the data presented and used in the evaluation of the recompression coefficients were based on experiments wherein boundary layer effects were small. However, the boundary layers in some of the cases, e.g. [18], could have been significant. These cases, however, were treated by determining values of the recompression coefficient which would improve case-by-case predicted-experimental agreement; the influence of boundary layers was apparently reflected by an increase in values of the recompression coefficient over values determined for those cases with negligible boundary layers. An alternative and possibly more attractive approach could be similar to that of [4,6]: Determining a recompression coefficient for negligible initial boundary layers and then accounting for the influence of boundary layers by "equivalent" mass and momentum "bleed" rates into the base region.

The recompression coefficient has been presented here as an empirical modification to the flow model of Korst, et al., which is intended solely to improve the engineering usefulness of computer programs based on this flow model. This correlation, while being quite useful, is not a satisfactory substitute for the much needed understanding of the fundamental controlling processes.

REFERENCES

1. Korst, H. H., Chow, W. L., and Zumwalt, G. W., "Research on Transonic and Supersonic Flow of a Real Fluid at Abrupt Increases in Cross Section (with Special Consideration of Base Drag Problems)--Final Report," University of Illinois Report No. ME-TN-392-5, December 1959, University of Illinois, Urbana, Illinois.

2. Addy. A. L., "Analysis of the Axisymmetric Base-Pressure and Base-Temperature Problem with Supersonic Interacting Freestream-Nozzle Flows Based on the Flow Model of Korst, et al., Part I: A Computer Program and Representative Results for Cylindrical Afterbodies," Report No. RD-TR-69-12, July 1969, U. S. Army Missile Command, Redstone Arsenal, Ala.

3. Nash, J. F., "An Analysis of Two-Dimensional Turbulent Base Flow, Including the Effect of the Approaching Boundary Layer," Reports and Memoranda No. 3344, 1963, Aeronautical Research Council, Ministry of Aviation, London, U. K.

4. Carrière, P., and Sirieix, M., "Résultats Récents dans l'Étude des Problèms de Mélange et de Recollement," T.P. No. 165, 1964, Office National d'Etudes et de Recherches Aérospatiales (ONERA), 29, Avenue de la Division Leclerc, Chatillon-sous-Bagneux (Seine), France (Also available as: Library Translation No. 1113, May 1965, Royal Aircraft Establishment, Ministry of Aviation, Farnborough, Hants, U.K.)

5. Page, R. H., Kessler, T. J., and Hill, W. G., Jr., "Reattachment of Two-Dimensional Supersonic Turbulent Flows," ASME Paper No. 67-FE-20, presented at ASME Fluids Engineering Conference, 1967, Chicago, Ill.

6. Sirieix, M., Délery, J., et Mirande, J., "Recherches Expérimentales Fondamentales sur les Écoulments Séparés et Applications," T.P. No. 520, 1967, Office National d'Etudes et de Recherches Aérospatiales (ONERA), 29, Avenue de la Division Leclerc-92, Chatillon, France.

7. Dixon, R. J., Richardson, J. M., and Page, R. H., "Turbulent Base Flow on an Axisymmetric Body with a Single Exhaust Jet," AIAA Paper No. 69-650, presented at AIAA Fluid and Plasma Dynamics Conference, 16-18 June 1969, San Francisco, Calif.

8. Cortright, E. M., Jr., and Schroeder, A. H., "Investigation at Mach Number 1.91 of Side and Base Pressure Distributions over Conical Boattails without and with Jet Flow Issuing from Base," NACA RM E51F26, Sept. 1951.

9. Messing, W. E., Rabb, L., and Disher, J. H., "Preliminary Drag and Heat-Transfer Data Obtained from Air-Launched Cone-Cylinder Test Vehicle over Mach Number Range from 1.5 to 5.18," NACA RM E53I04, Nov. 1953.

10. Bromm, A. F., Jr., and O'Donnell, R. M., "Investigation at Supersonic Speeds of the Effect of Jet Mach Number and Divergence Angle of the Nozzle upon the Pressure of the Base Annulus of a Body of Revolution," NACA RM L54I16, Dec. 1954.

11. Baughman, L.E. and Kochendorfer, F. D., "Jet Effects on Base Pressures of Conical Afterbodies at Mach 1.91 and 3.12," NACA RM E57E06, Aug. 1957.

12. Reid, J., and Hastings, R. C., "The Effect of a Control Jet on Base Pressure of a Cylindrical Afterbody in a Supersonic Stream," Report No. Aero 2621, Dec. 1959, Royal Aircraft Establishment, Farnborough, England.

13. Henderson, J. H., "Jet Effects on Base Pressures of Cylindrical and Flared Afterbodies at Free-Stream Mach Numbers of 1.65, 1.82, and 2.21," ARGMA TR 1G3R, June 1960, Army Rocket and Guided Missile Agency, Ordnance Missile Laboratories Division, System Analysis Laboratory, Redstone Arsenal, Ala.

14. Craven, A. H., Chester, D. H., and Graham, B. H., "Base Pressure at Supersonic Speeds in the Presence of a Supersonic Jet," CoA Report No. 144, AD No. 260621, Dec. 1960, The College of Aeronautics, Cranfield, U.K.

15. Charczenko, N. and Hayes, C., "Jet Effects at Supersonic Speeds on Base and Afterbody Pressures of a Missile Model Having Single and Multiple Jets," NASA TN D-2046, Nov. 1963, Langley Research Center, Hampton, Va.

16. Roberts, J. B., and Golesworthy, G. T., "An Experimental Investigation of the Influence of Base Bleed on the Base Drag of Various Propelling Nozzle Configurations," Aeronautical Research Council (U.K.), Current Papers, C. P. No. 892, 1966.

17. White, W. E., "Effect of Base Bleed Exit Area on Base Drag with Simulated Rocket Exhaust at Mach Numbers 2.5, 3.0, and 3.5," AEDC-TR-66-246, Dec. 1966, PWT, Arnold Engineering Development Center, Arnold Air Force Station, Tennessee.

18. Harries, M. H., "Pressure on Axisymmetric Base in a Transonic or Supersonic Free Stream in the Presence of a Jet," Report 111, March 1967, FFA (The Aeronautical Research Institute of Sweden), Stockholm, Sweden.

19. Reid, J., "The Effect of Jet Temperature on Base Pressure," Royal Aircraft Establishment Technical Report 68176, July 1968.

20. Brazzel, C. E., "Unpublished Base-Pressure Data Obtained by the Aerodynamics Branch (AMSMI-RDK)," Advanced System Laboratory, U. S. Army Missile Command, Redstone Arsenal, Ala.

21. Lilienthal, P. F. II, Brink, D. F., and Addy, A. L., "An Investigation of Factors Influencing the Annular Base Drag of Bodies of Revolution with Jet Flow in Transonic and Supersonic External Streams," (in preparation) U. S. Army Missile Command Contract No DA-01-021-AMC-13902(Z), University of Illinois at Urbana-Champaign, Urbana, Ill.

TABLE I

Reference	Data†	M_{1E}	M_{1I}	β_{1I}	$\bar{R}_{1I}$	r	Comparison Fig. No.
[8] Cortright and Schroeder	---	1.91	1.0	0°	0.5	0.841	4
[9] Messing, Rabb, and Disher	$\bar{T}_{oE} = 0.141$ $\gamma_I = 1.22$	1.5 to 5.15	2.93	15°	0.555	0.875	5
[10] Bromm and O'Donnell	---	1.62, 1.94, 2.41	1.0	0°	0.5	0.840	6a
					0.75	0.934	
		1.62	3.0	0°,10°,20°	0.75	1.0	6b
		1.94		0°	0.75	1.0	6c
				10°		0.960	
[11] Baughman and Kochendorfer	---	1.91, 3.12	1.0	0°	0.375	0.782	7
[12] Reid and Hastings	---	2.0	2.0	0°,5°	0.8	0.95	8
				0°,5°,10°	0.6	0.85	
				0°,5°	0.4	0.8	
				0°,5°	0.2	0.7	

†Unless otherwise noted, the following variables are the same for all configurations and have the values:

$R_E = R_I = 53.35 (lb_f\text{-ft}/lb_m\text{-}°R)$ $\quad \bar{X}_{1E} = \bar{X}_{1I} = 0.0$ $\quad \bar{T}_{oE} = 1.0$

$\gamma_E = \gamma_I = 1.4$ $\quad \bar{R}_{1E} = 1.0$ $\quad \bar{B}_o = \bar{E}_o = 0.0$

TABLE I (continued)

Reference	Data†	M_{1E}	M_{II}	β_{II}	$\bar{R}_{II}$	r	Comparison Fig. No.
[13] Henderson	---	1.65	2.5	15°	0.333	0.759	9a
					0.455	0.821	
		1.82		0°	0.333	0.825	9b
					0.455	0.900	
				15°	0.333	0.755	9c
					0.455	0.850	
		2.21		0°	0.333	0.755	9d
					0.455	0.875	
				15°	0.333	0.825	9e
					0.455	0.900	
[14] Craven. et al.	---	2.0	1.0, 1.4, 2.0	0°	0.188	0.625	10
[15] Charczenko and Hayes	$\bar{X}_{II} = 1.0$	2.3, 2.95 4.0, 4.65	3.19	10°	0.437	0.813	11
[16] Roberts and Golesworthy	$0 \leq \bar{B}_o \leq 0.06$	2.20	2.23	10°	0.772	0.941	12
[17] White	$0 \leq \bar{B}_o \leq 0.08$ $P_{oI}/P_{1E} = 30$	2.5	2.7	20°	0.20	0.660	13a
	$0 \leq \bar{B}_o \leq 0.06$ $P_{oI}/P_{1E} = 112$						13b

TABLE I (continued)

Reference	Data†	M_{1E}	M_{11}	β_{11}	$\bar{R}_{11}$	r	Comparison Fig. No.
[18] Harries	---	1.5	1.0	0°	0.333	0.800	14a
		2.01					
		1.5	1.5	10°	0.200	0.720	14b
[19] Reid	$0.333 \leq \bar{T}_{oE} \leq 1.0$ $1.33 \leq \gamma_1 \leq 1.4$ $R_1 = 97$ lb_f-ft/lb_m-°R	2.0	1.0	0°	0.5	0.780	15a
			2.0	0°	0.645	0.897	15b
[20] Brazzel	---	2.5	1.0	0°	0.2	0.650	16a
					0.141	0.625	
					0.1	0.588	
			1.78	20°	0.3	0.675	16b
					0.2	0.625	
					0.1	0.575	
			2.7	20°	0.3	0.74	16c
					0.2	0.672	
					0.1	0.588	
					0.3	0.74	16d

TABLE I (continued)

Reference	Data†	M_{1E}	M_{11}	β_{11}	$\bar{P}_{11}$	r	Comparison Fig. No.
[20] Brazzel	---	3.0	1.0	0°	0.2	0.625	16e
					0.141	0.590	
					0.1	0.588	
			1.78	20°	0.3	0.645	16f
					0.2	0.590	
					0.1	0.588	
			2.7	20°	0.3	0.720	16g
					0.2	0.672	
		2.5	1.0	0°	0.45	0.819	16h
		2.87			0.45	0.819	
		1.5	2.7	0°	0.8	0.951	16i
				20°	0.8	0.951	
		2.5		0°	0.8	0.951	16j
				10°	0.8	0.951	
			3.8	20°	0.8	0.951	16ℓ

TABLE I (continued)

Reference	Data†	M_{1E}	M_{11}	β_{11}	$\bar{P}_{11}$	r	Comparison Fig. No.
[21] U. of Ill. U-C	---	2.0	1.0	0°	0.125	0.611	
					0.141	0.624	
					0.175	0.652	
					0.200	0.672	
					0.250	0.708	17a
			1.78	0°	0.168	0.647	
					0.210	0.679	
					0.250	0.708	
				5°	0.200	0.672	
					0.250	0.708	
				20°	0.100	0.588	
					0.125	0.611	
					0.200	0.672	
					0.250	0.708	17a
					0.300	0.740	
					0.375	0.782	
			2.2	0°	0.200	0.672	
					0.250	0.708	
				20°	0.200	0.672	
					0.250	0.708	
			2.7	0°	0.200	0.672	
					0.250	0.708	

TABLE I (continued)

Reference	Data†	M_{1E}	M_{11}	β_{11}	$\bar{R}_{11}$	r	Comparison Fig. No.
[21] U. of Ill. U-C	---	2.0	2.7	0°	0.252	0.709	
					0.314	0.749	
				10°	0.200	0.672	
					0.250	0.708	
				20°	0.200	0.672	
					0.250	0.709	17b
					0.300	0.740	
					0.375	0.782	
			3.2	0°	0.200	0.672	
					0.250	0.708	
					0.320	0.752	
					0.400	0.795	
				20°	0.200	0.672	
					0.250	0.708	17a
			3.8	20°	0.200	0.672	
					0.250	0.709	
		2.5	1.0	0°	0.241	0.624	
					0.300	0.708	
			1.78	0°	0.248	0.647	
				5°	0.300	0.693	

TABLE I (continued)

Reference	Data†	M_{1E}	M_{11}	β_{11}	$\bar{R}_{11}$	r	Comparison Fig. No.
[21] U. of Ill. U-C	---	2.5	1.78	20°	0.100	0.588	
					0.200	0.672	
					0.300	0.740	
			2.2	0°	0.200	0.672	
				20°	0.200	0.672	
			2.7	0°	0.200	0.672	
					0.252	0.709	
				10°	0.200	0.672	
				15°	0.200	0.672	
				20°	0.200	0.672	
					0.300	0.740	
			3.2	0°	0.200	0.672	
					0.320	0.752	
				20°	0.200	0.672	
			3.8	20°	0.200	0.672	
	Freon 14 $\gamma_1 = 1.22$	2.0	2.44	20°	0.250	0.708	17b
			2.80	20°	0.250	0.708	
			3.20	20°	0.250	0.708	

TABLE I (continued)

Reference	Data†	M_{1E}	M_{11}	β_{11}	$\bar{R}_{11}$	r	Comparison Fig. No.
[21] U. of Ill. U-C	Helium $\gamma_1 = 1.67$	2.0	1.0	0°	0.125	0.611	
					0.250	0.706	
			1.88	5°	0.250	0.708	
				20°	0.250	0.708	
			2.41	20°	0.250	0.708	
			3.09	20°	0.250	0.708	17b
				20°	0.375	0.782	
			3.89	20°	0.250	0.708	

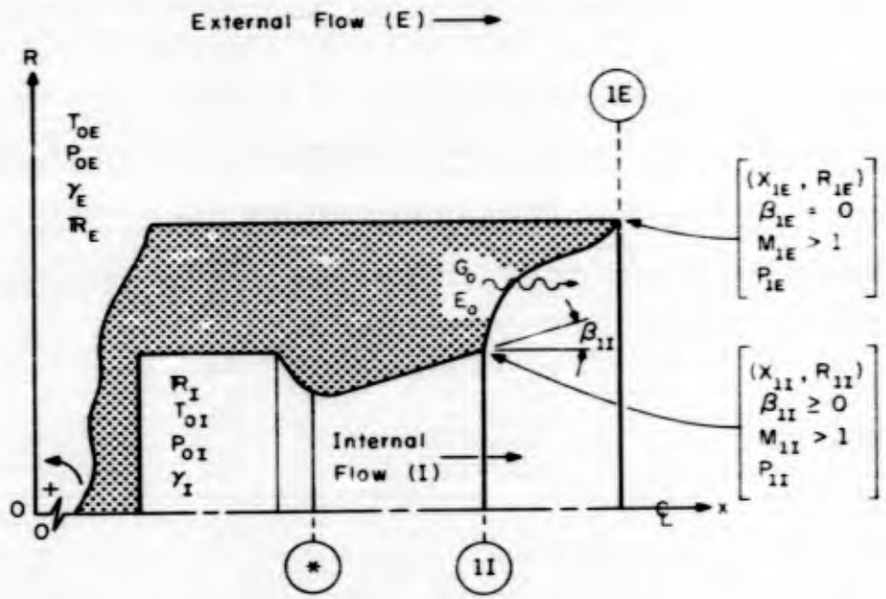

Figure 1. Two-Stream Axisymmetric Base-Flow Configuration and Notation

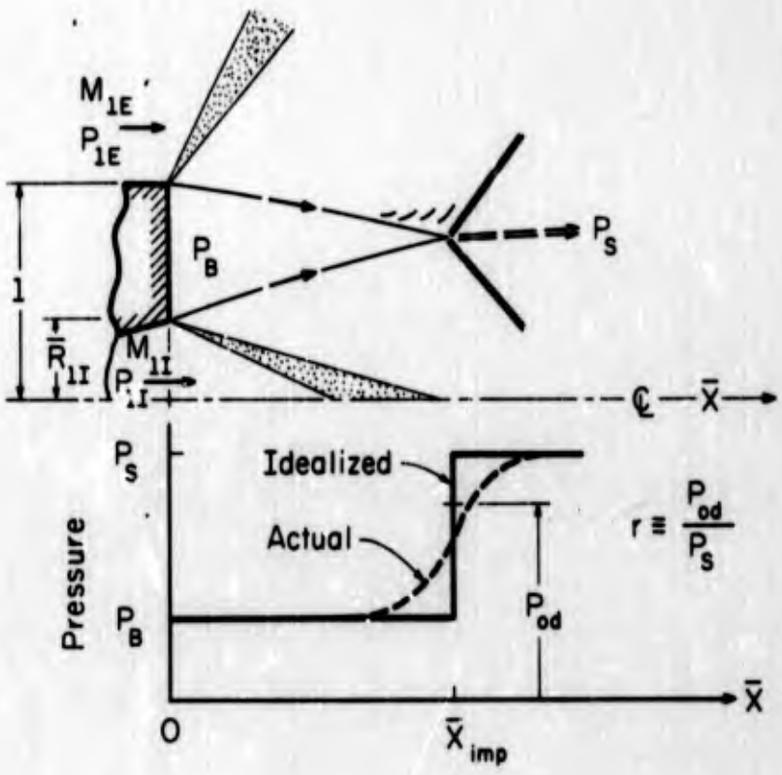

Figure 2. Definition of the Empirical Recompression Coefficient

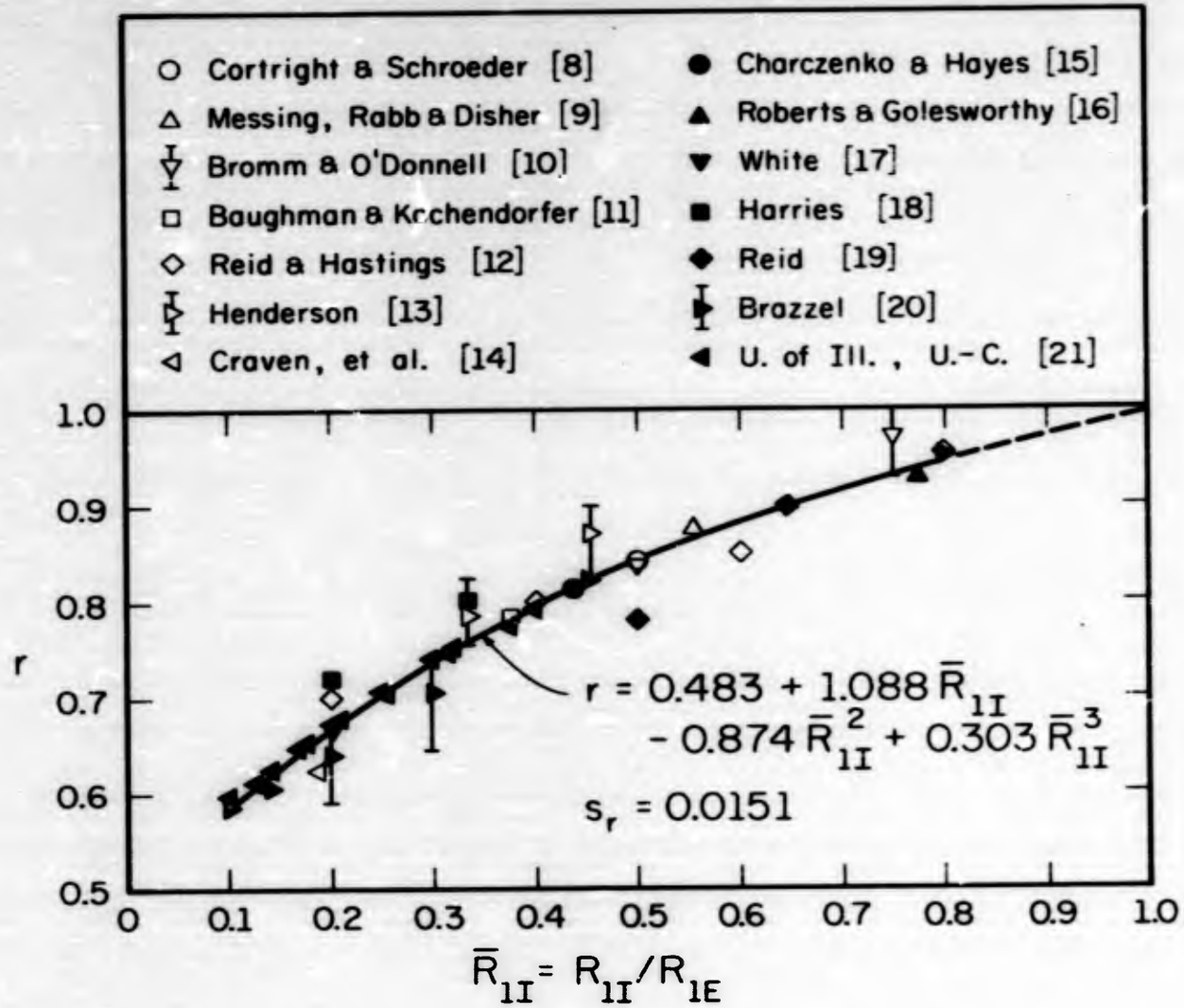

Figure 3. Functional Behavior of the Recompression Coefficient

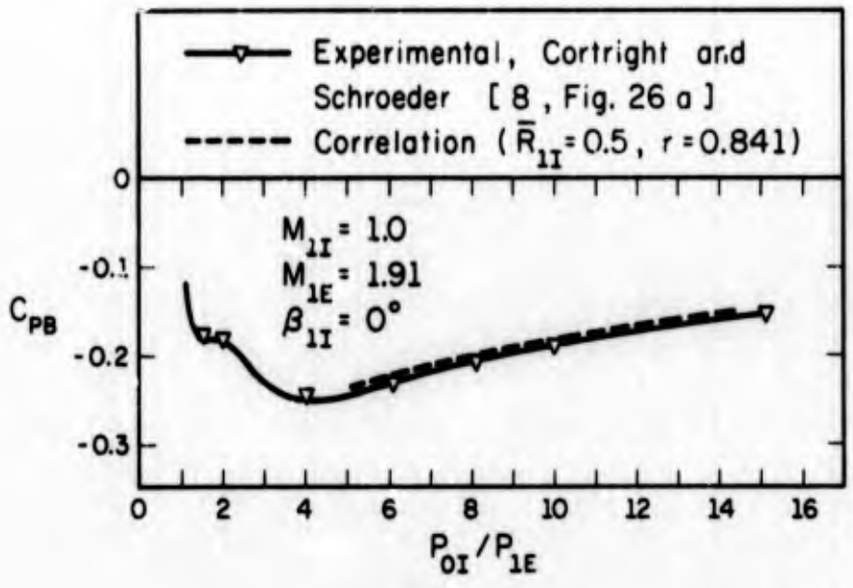

Figure 4. A Comparison with the Data of Cortright and Schroeder [8]

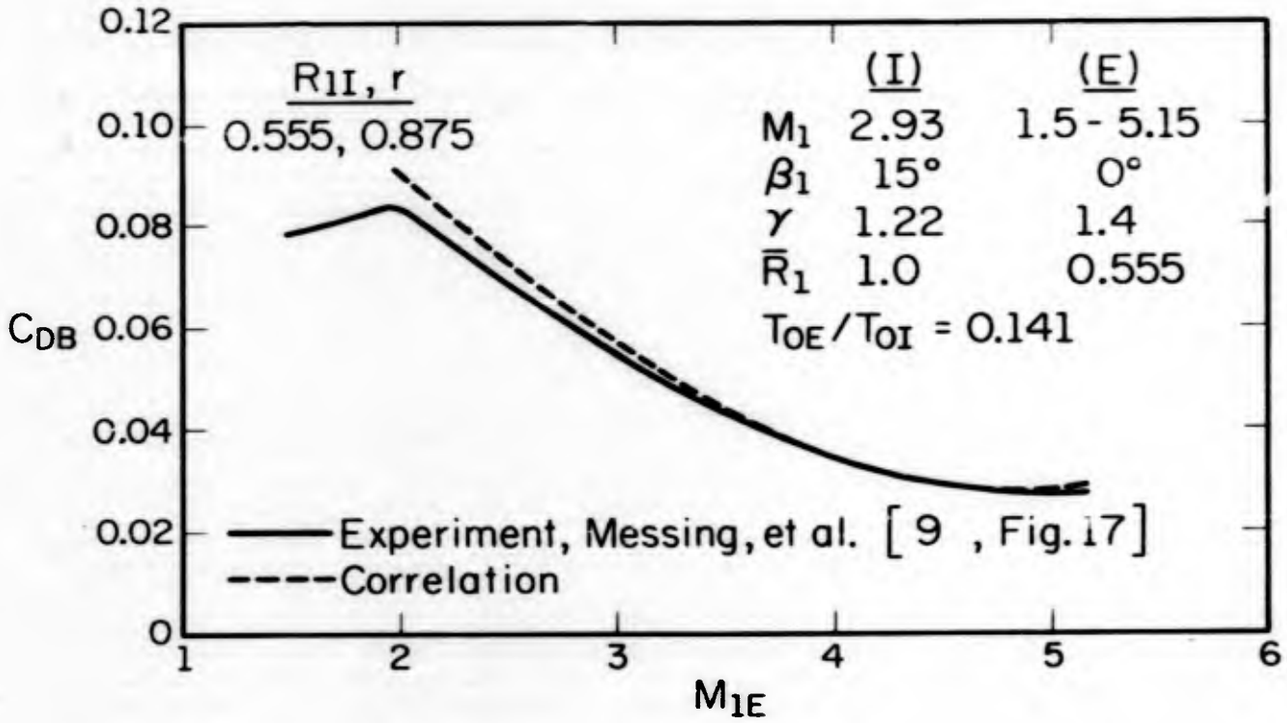

Figure 5. A Comparison with the Data of Messing, et al. [9]

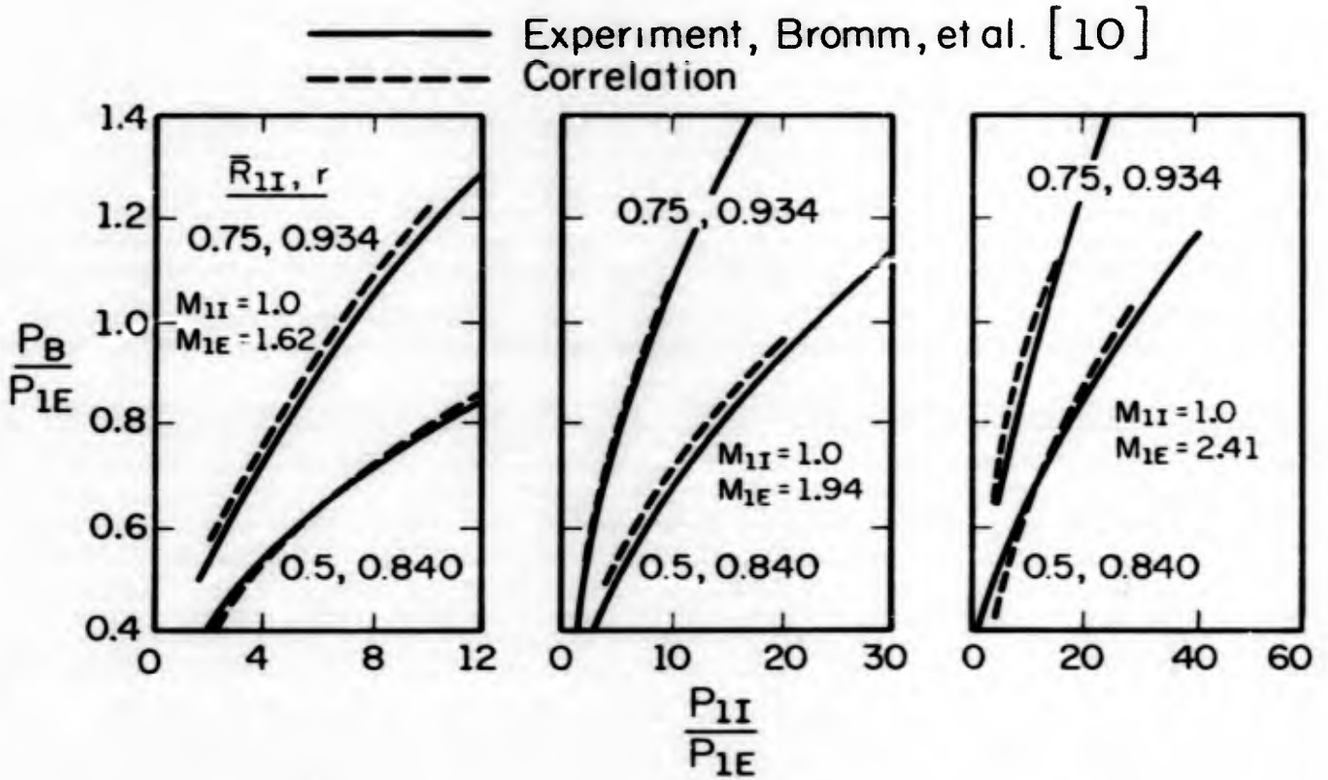

(a) Variations in $\bar{R}_{1I}$ and M_{1E}

Figure 6. A Comparison with the Data of Bromm, et al. [10]

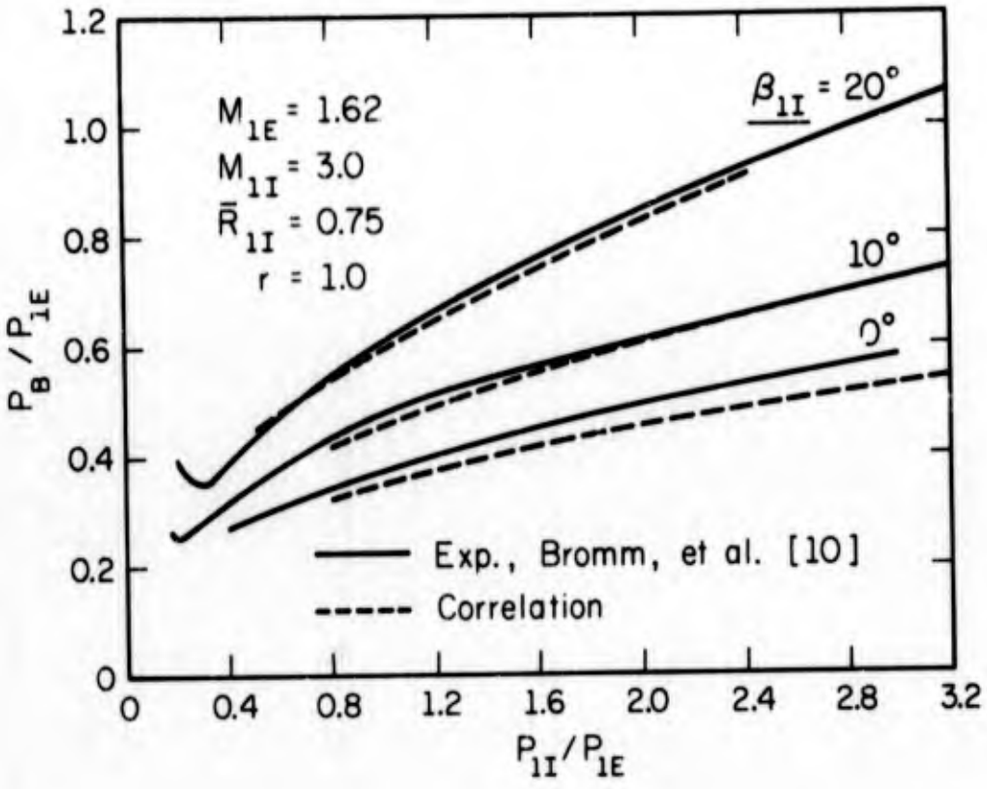

(b) Variations in β_{1I} (M_{1I} = 3, M_{1E} = 1.62, $\bar{R}_{1I}$ = 0.75)

Figure 6. continued

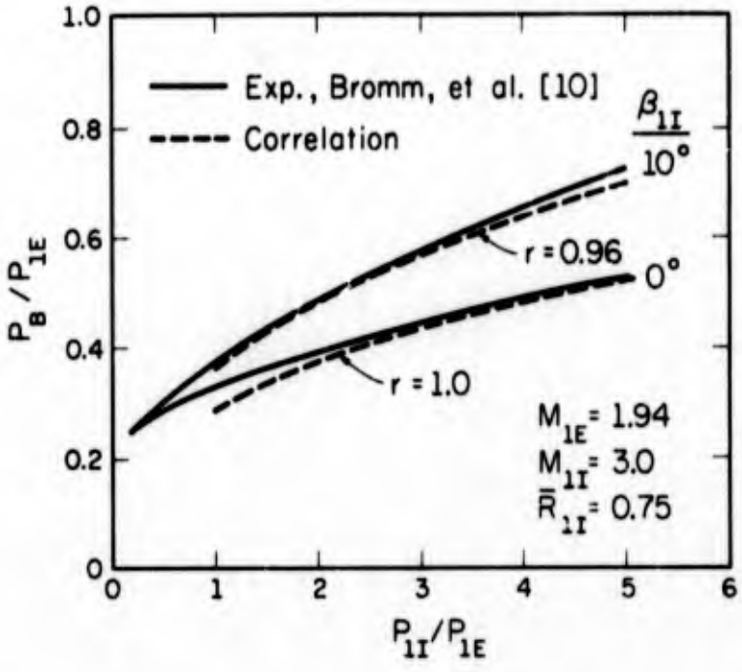

(c) Variations in β_{1I} (M_{1I} = 3, M_{1E} = 1.94, $\bar{R}_{1I}$ = 0.75)

Figure 6. continued

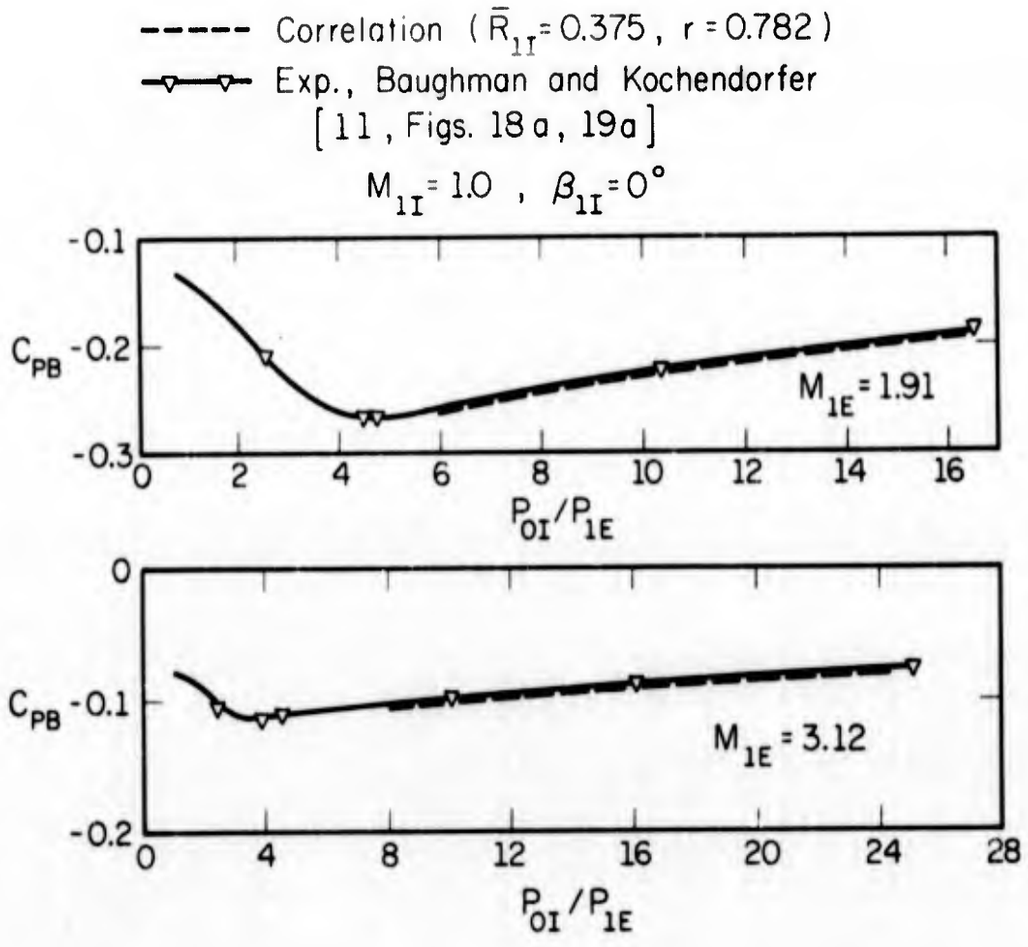

Figure 7. A Comparison with the Data of Baughman and Kochendorfer [11]

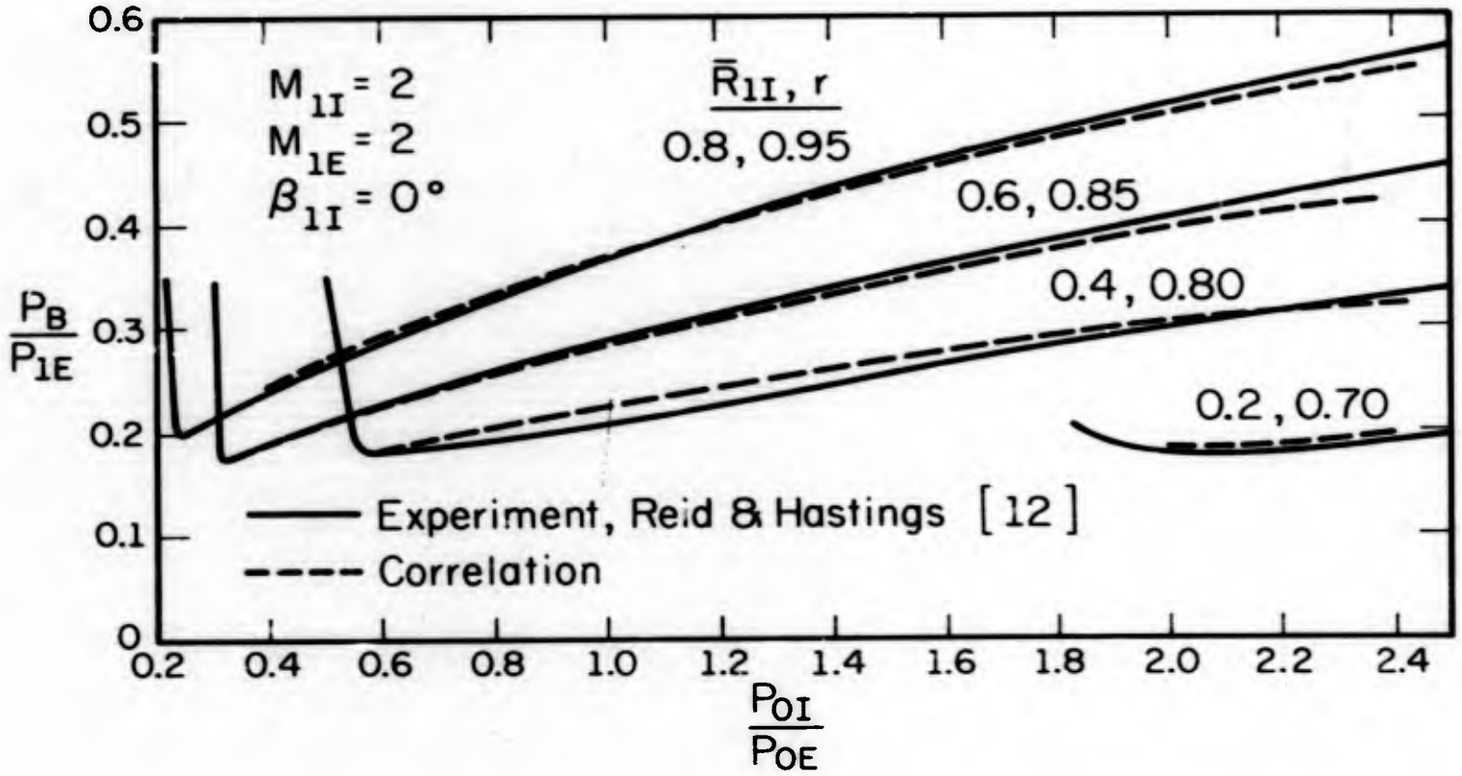

Figure 8. A Comparison with the Data of Reid and Hastings [12]

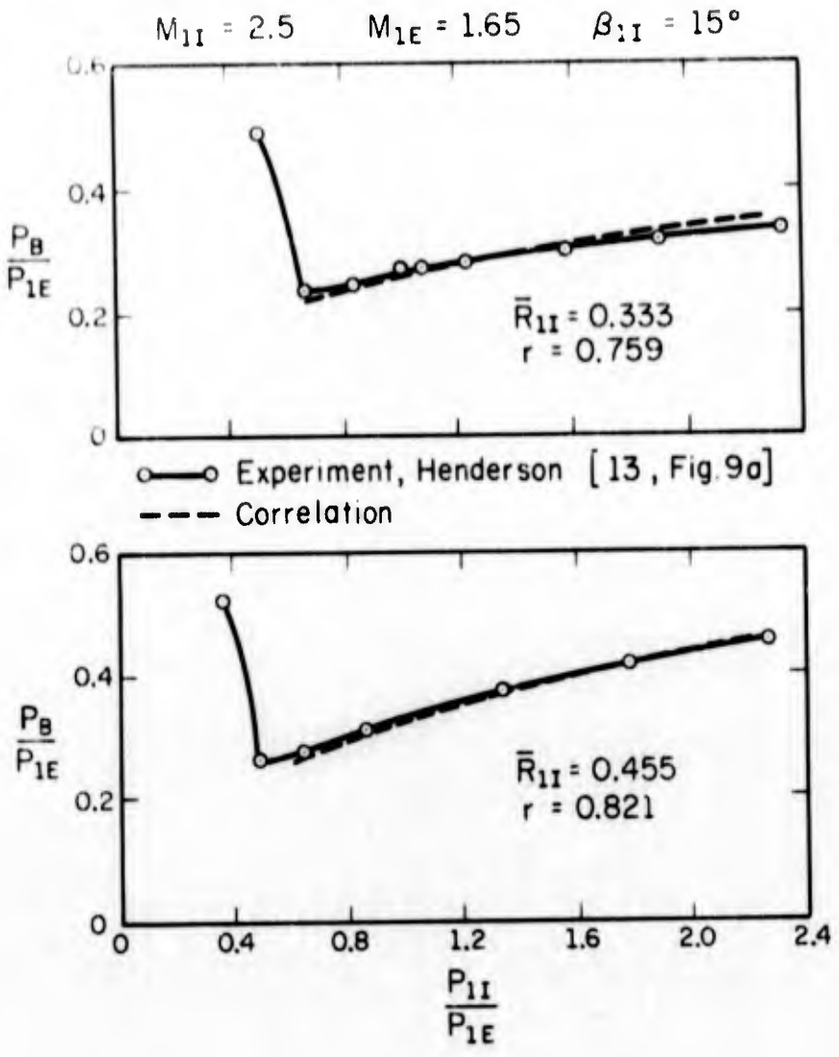

(a) Variations in $\bar{R}_{1I}$ (M_{1E} = 1.65, β_{1I} = 15°)

Figure 9. A Comparison with the Data of Henderson [13]

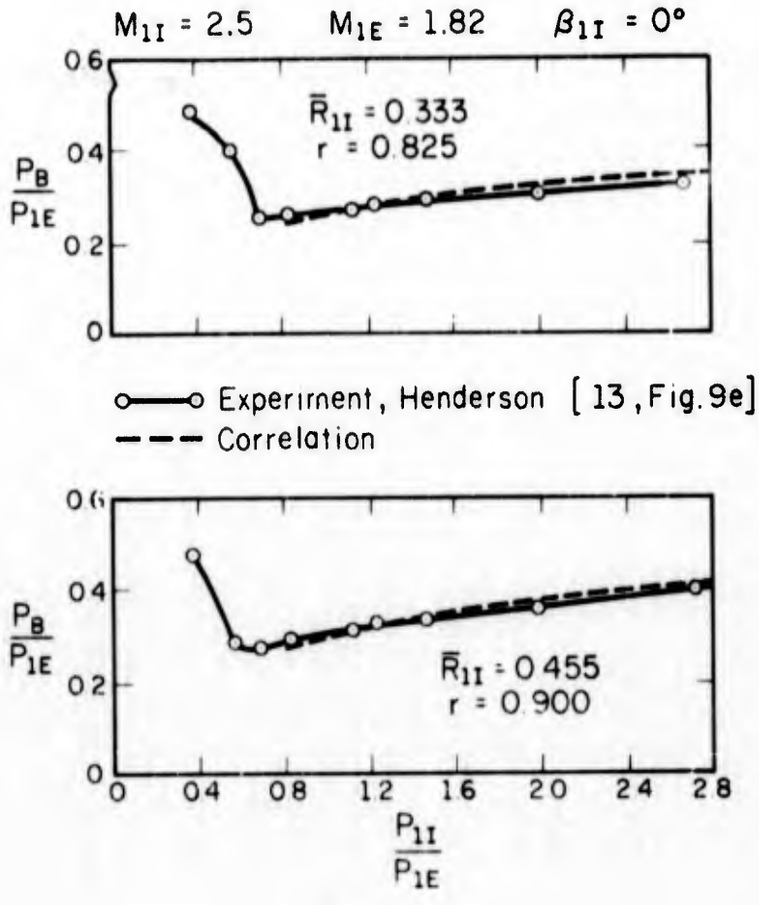

(b) Variations in $\bar{R}_{1I}$ (M_{1E} = 1.82, β_{1I} = 0°)

Figure 9. continued

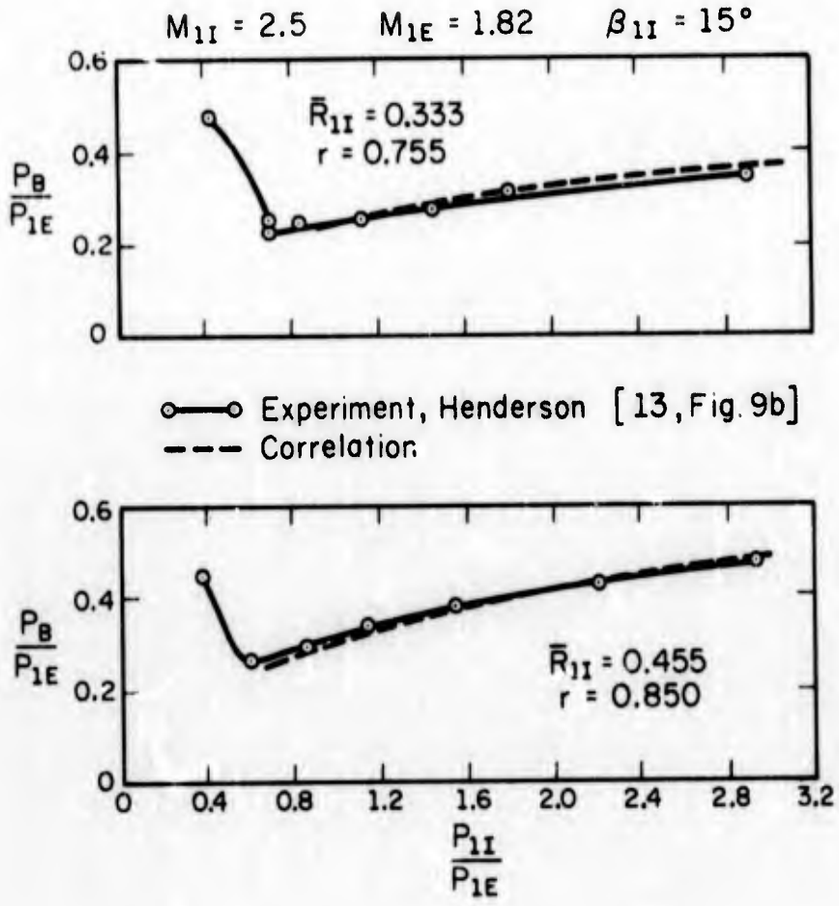

(c) Variations in $\bar{R}_{1I}$ (M_{1E} = 1.82, β_{1I} = 15°)

Figure 9. continued

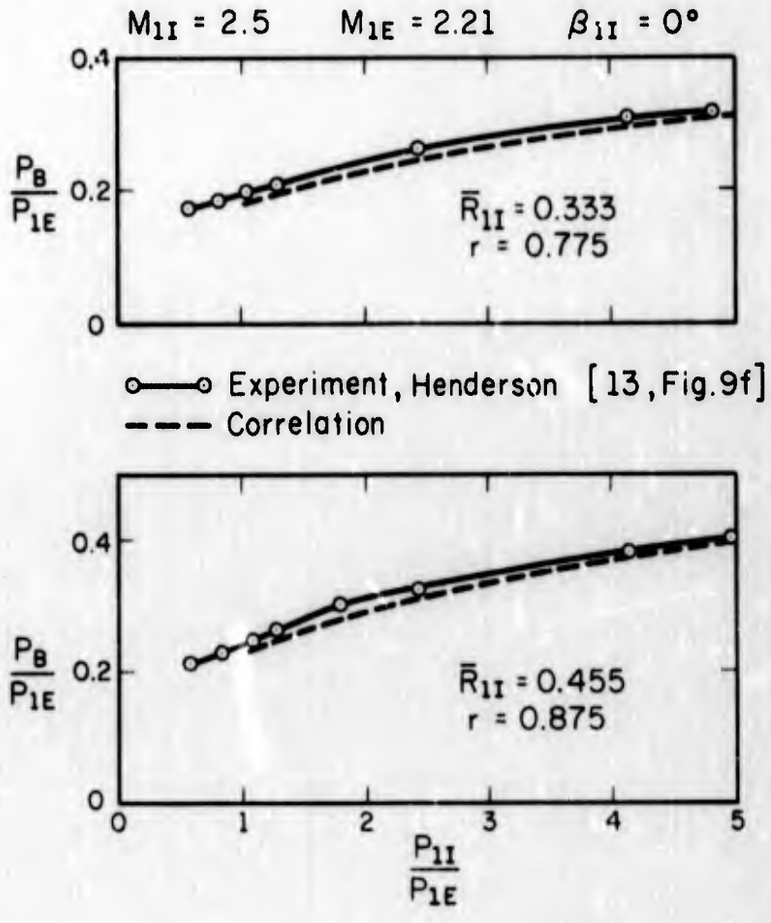

(d) Variations in $\bar{R}_{1I}$ (M_{1E} = 2.21, β_{1I} = 0°)

Figure 9. continued

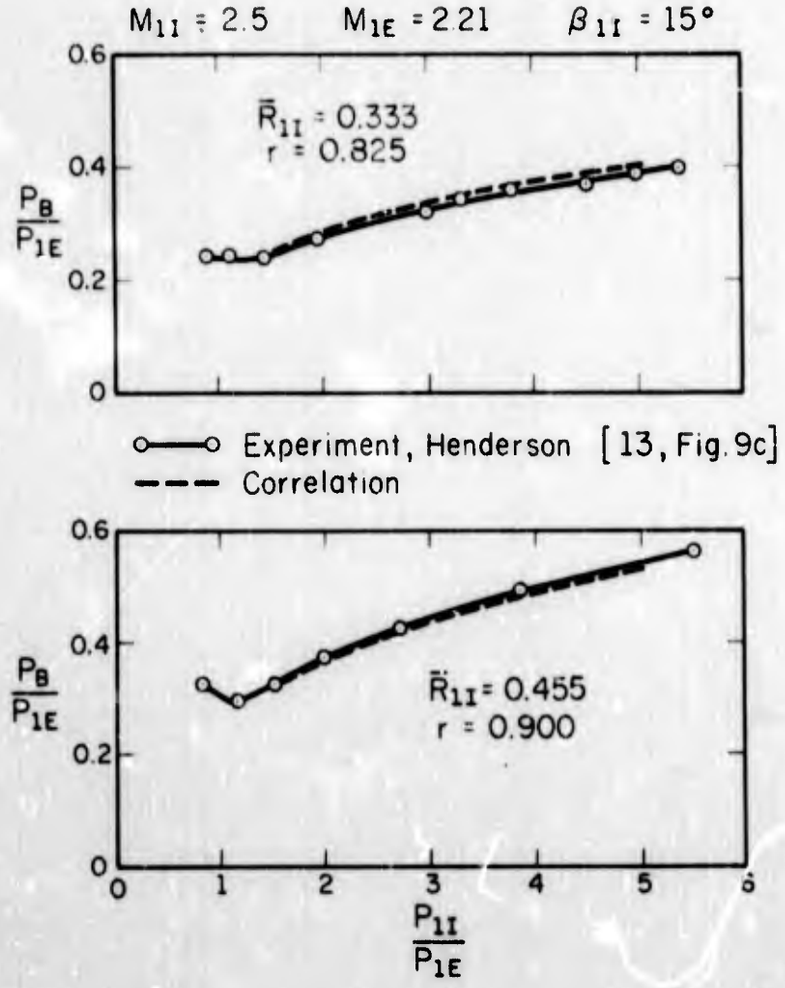

(e) Variations in $\bar{R}_{1I}$ (M_{1E} = 2.21, β_{1I} = 15°)

Figure 9. continued

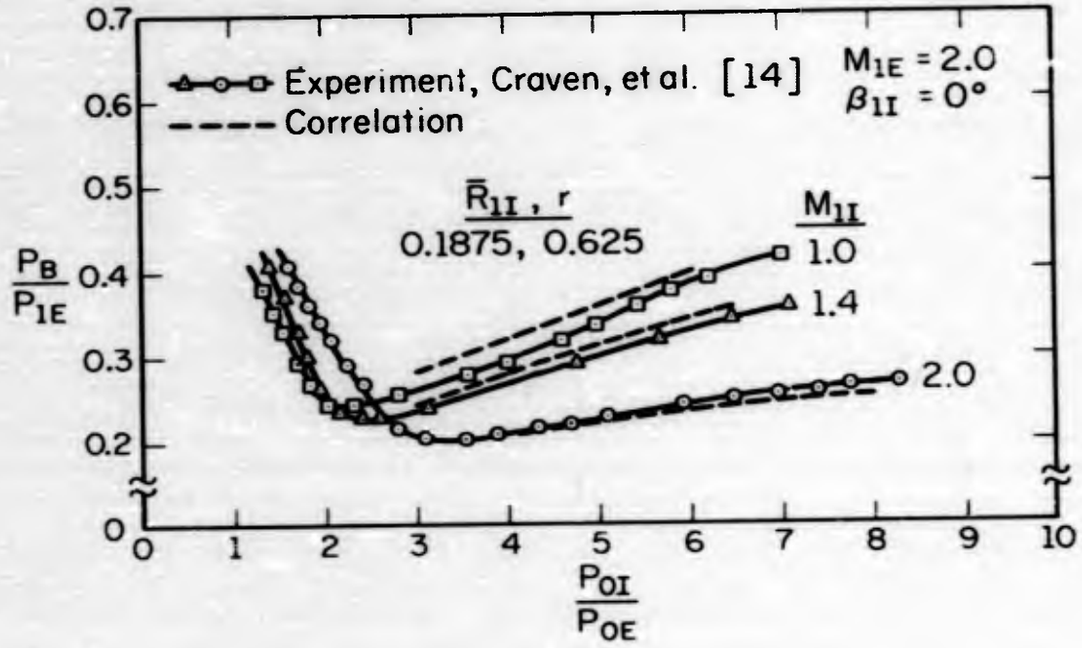

Figure 10. A Comparison with the Data of Craven, et al. [14]

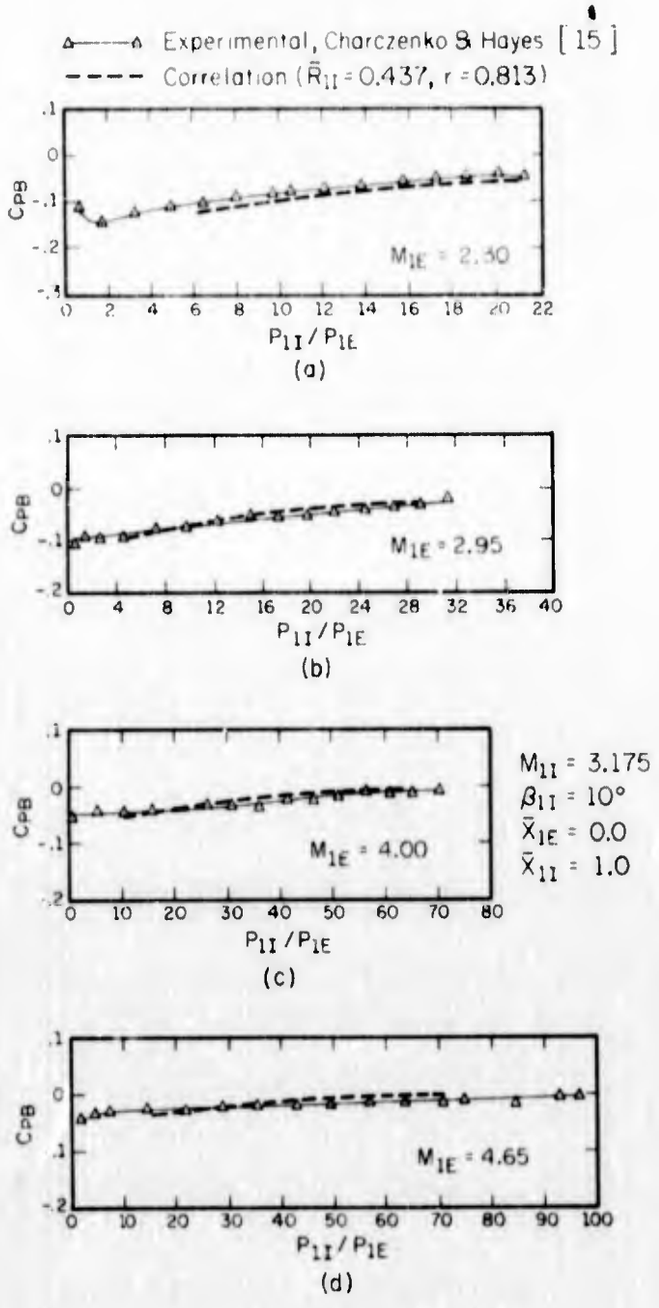

Figure 11. A Comparison with the Data of Charczenko and Hayes [15]

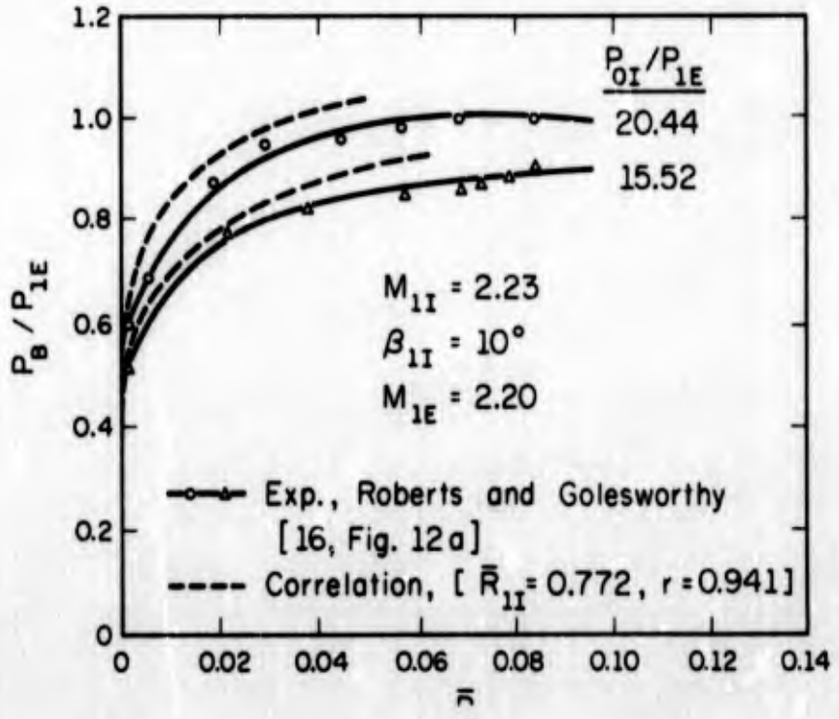

Figure 12. A Comparison with the Data of Roberts and Golesworthy [16]

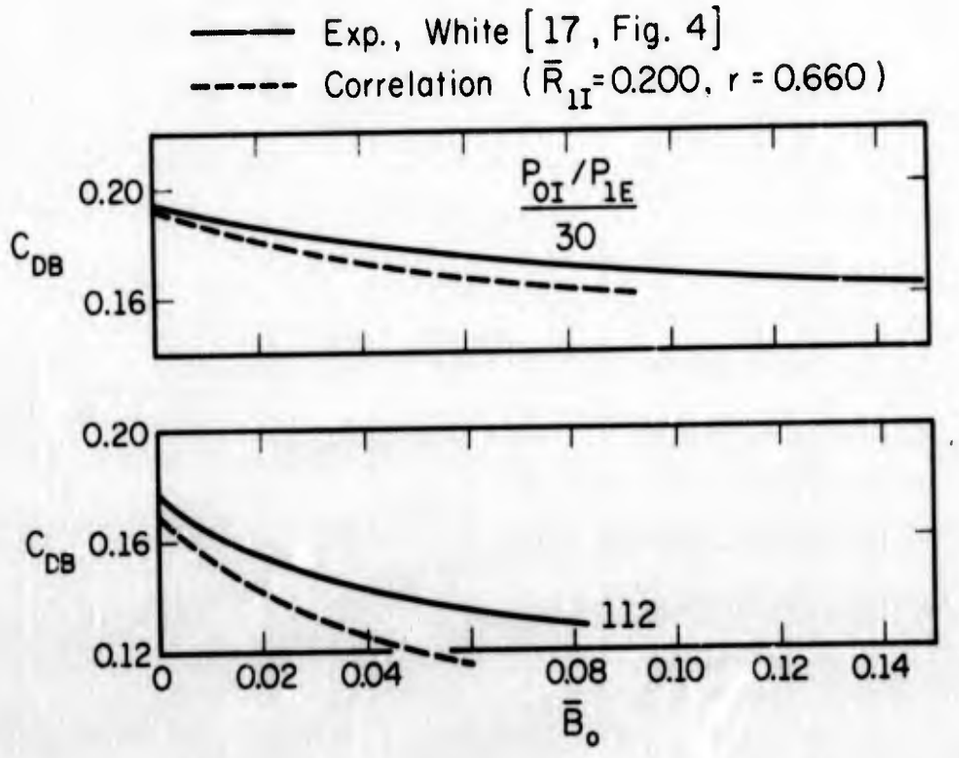

Figure 13. A Comparison with the Data of White [17]

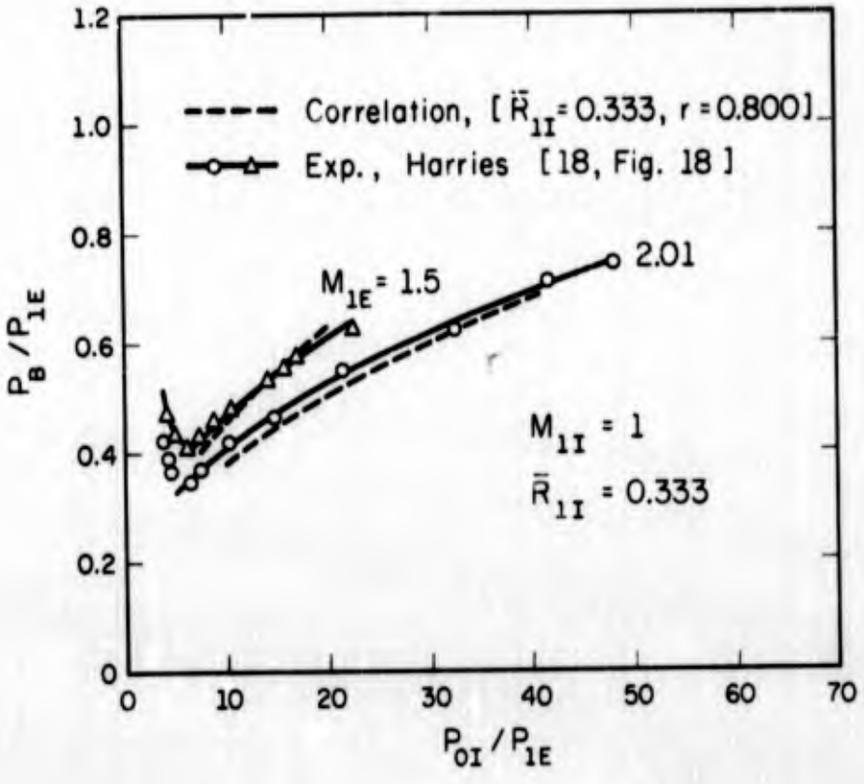

(a) Variations in M_{1E}

Figure 14. A Comparison with the Data of Harries [18]

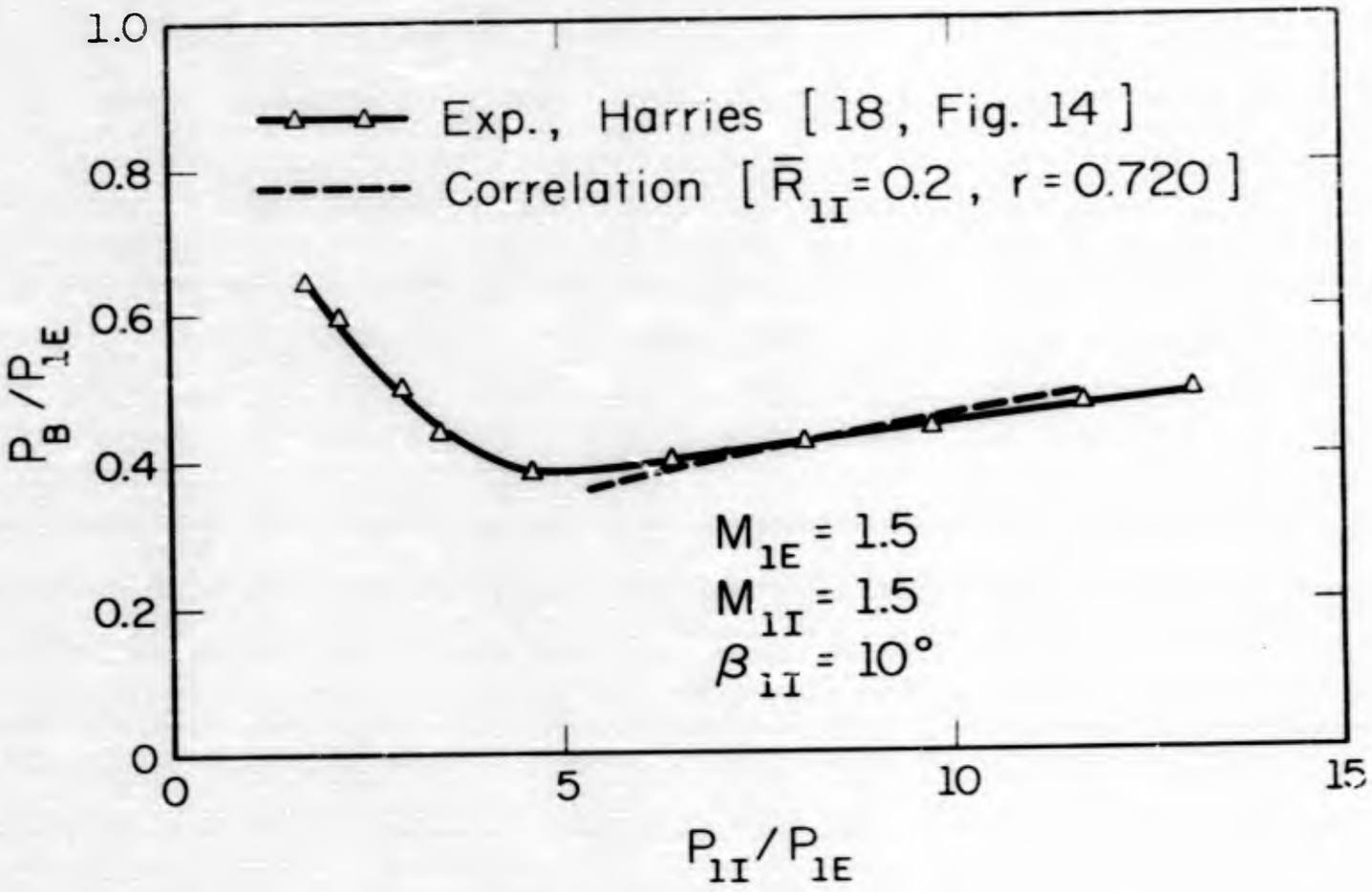

(b) Variation in P_{1I}/P_{1E}

Figure 14. continued

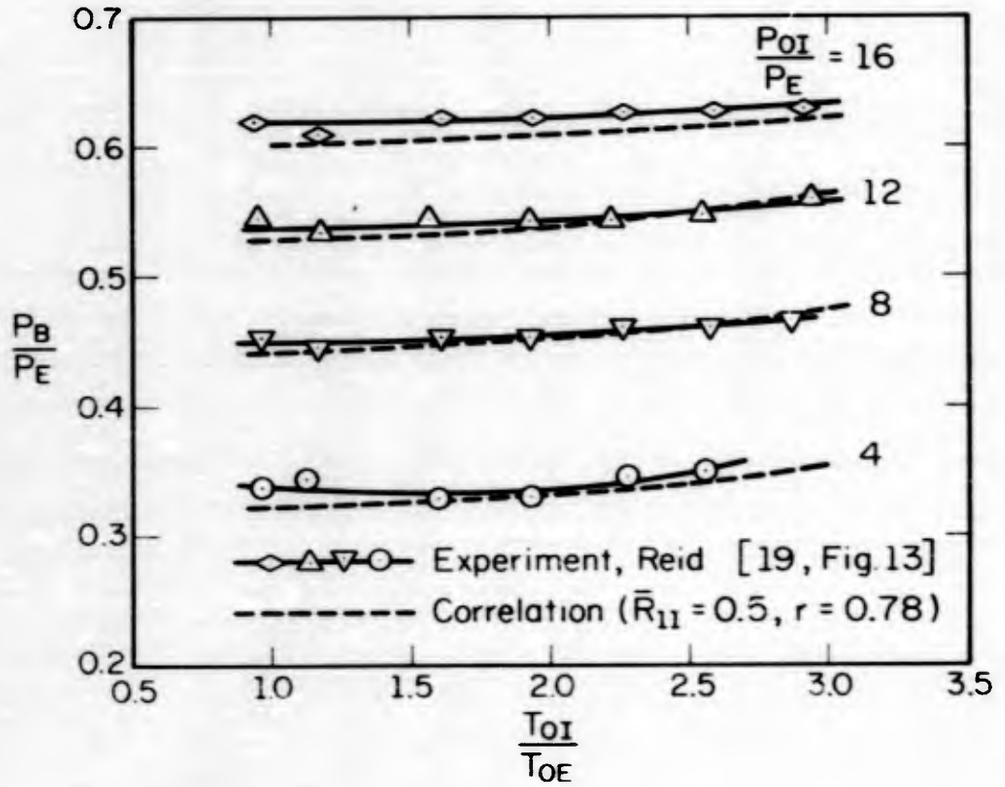

(a) Variation in T_{oI}/T_{oE} for given Values of P_{oI}/P_E ($\bar{R}_{11}$ = 0.5)

Figure 15. A Comparison with the Data of Reid [19]

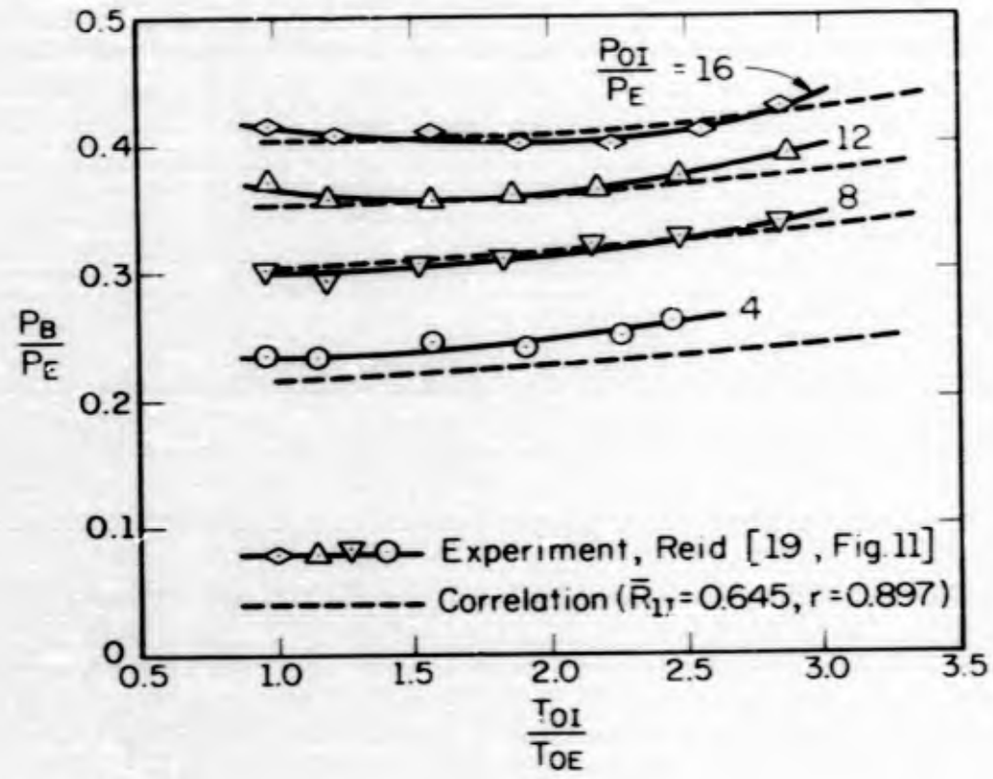

(b) Variation in T_{oI}/T_{oE} for given Values of P_{oI}/P_E ($\bar{R}_{11}$ = 0.645)

Figure 15. continued

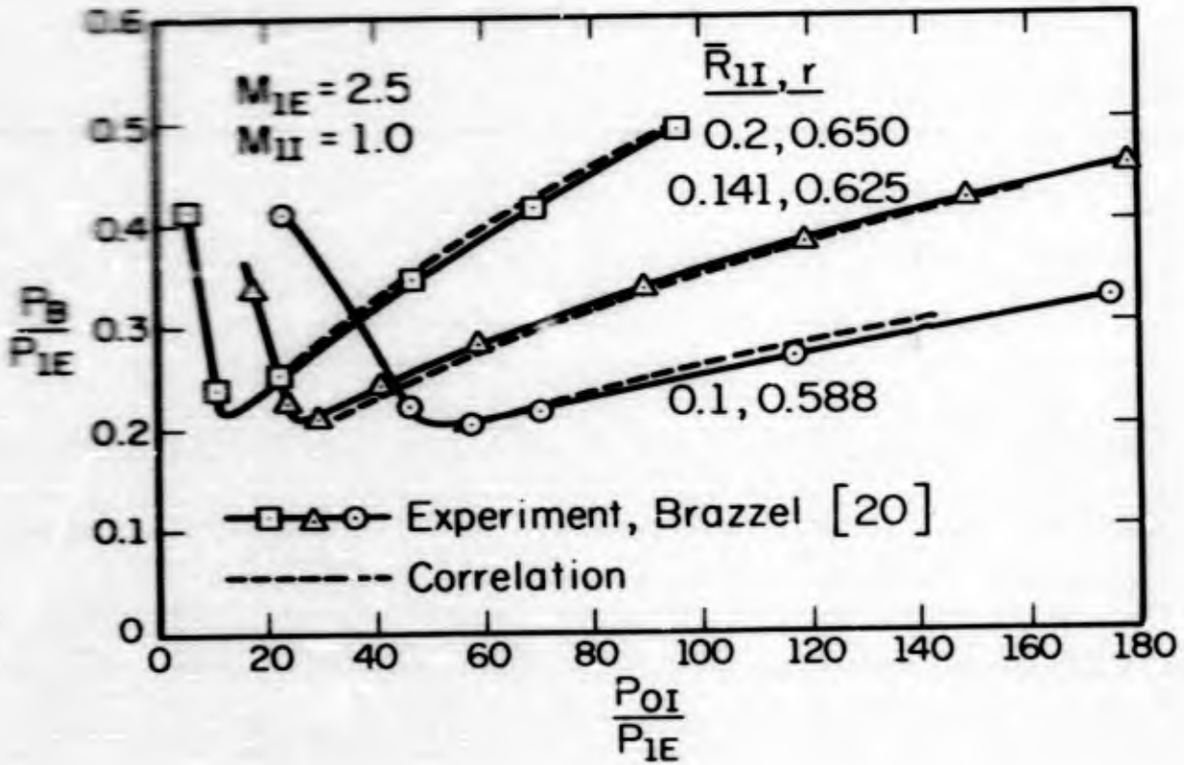

(a) Variations in $\bar{R}_{1I}$ ($M_{1E} = 2.5$, $M_{1I} = 1.0$)

Figure 16. A Comparison with the Data of Brazzel [20]

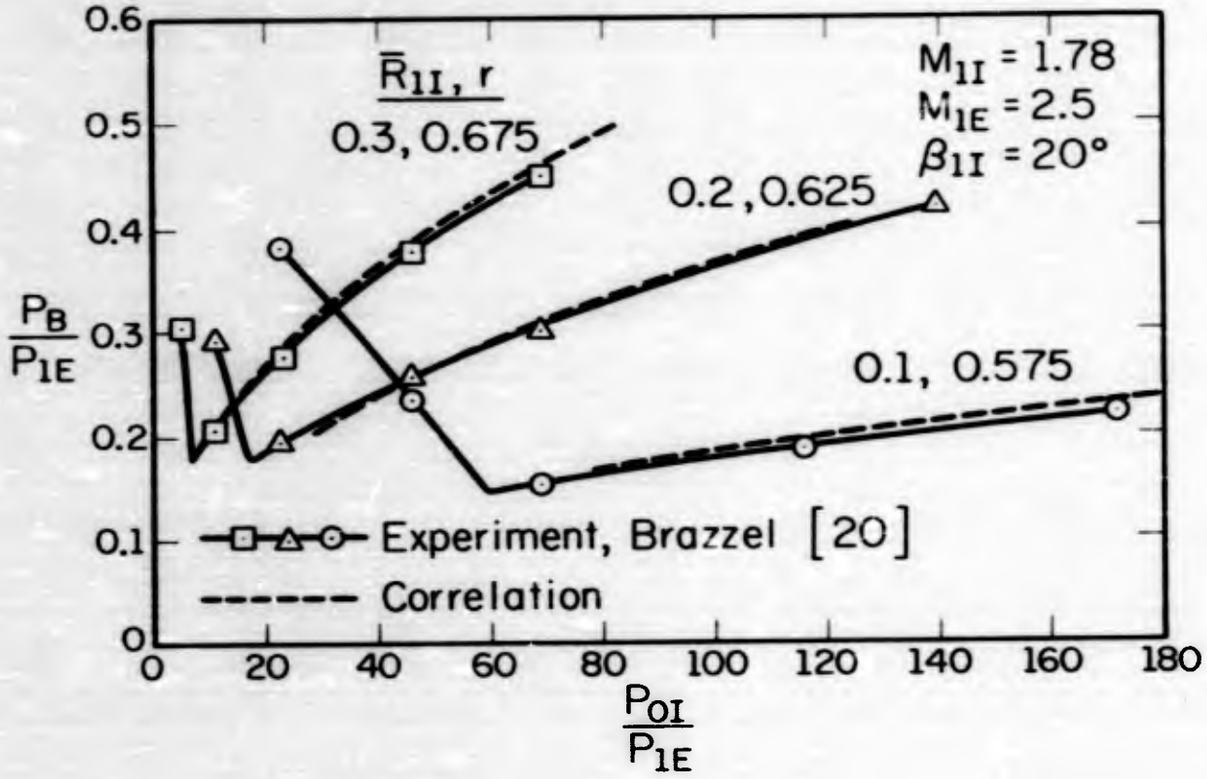

(b) Variations in $\bar{R}_{1I}$ (M_{1E} = 2.5, M_{1I} = 1.78, β_{1I} = 20°)

Figure 16. continued

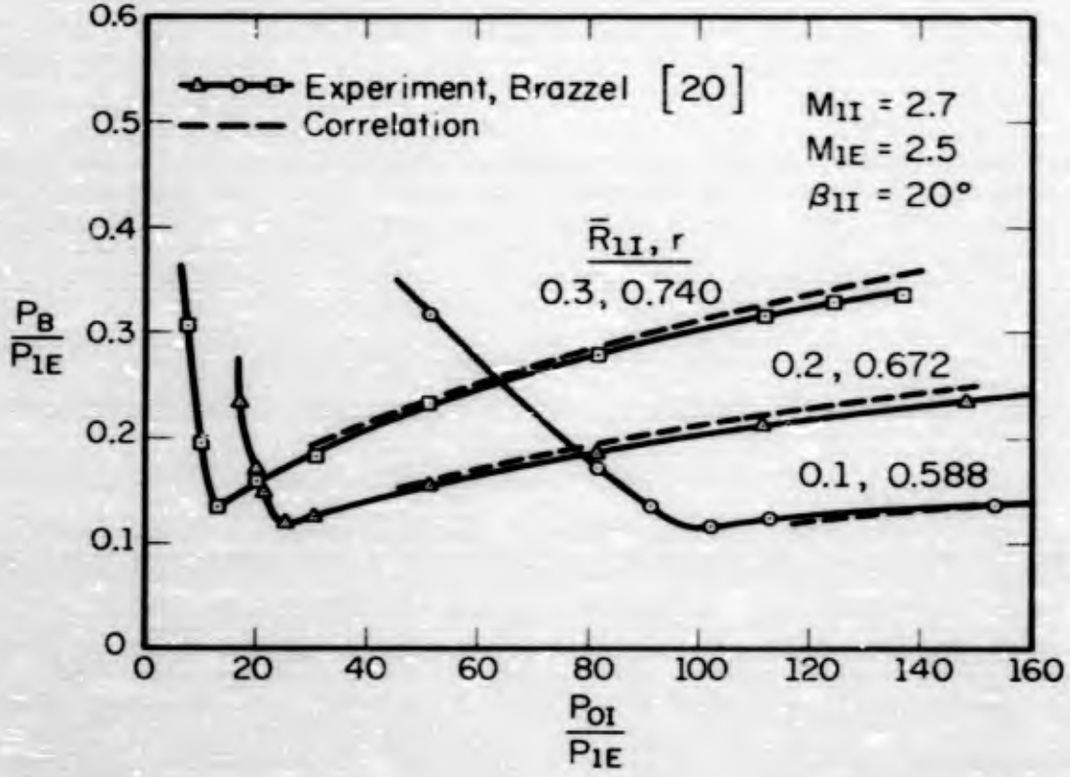

(c) Variations in $\bar{R}_{1I}$ (M_{1E} = 2.5, M_{1I} = 2.7, β_{1I} = 20°)

Figure 16. continued

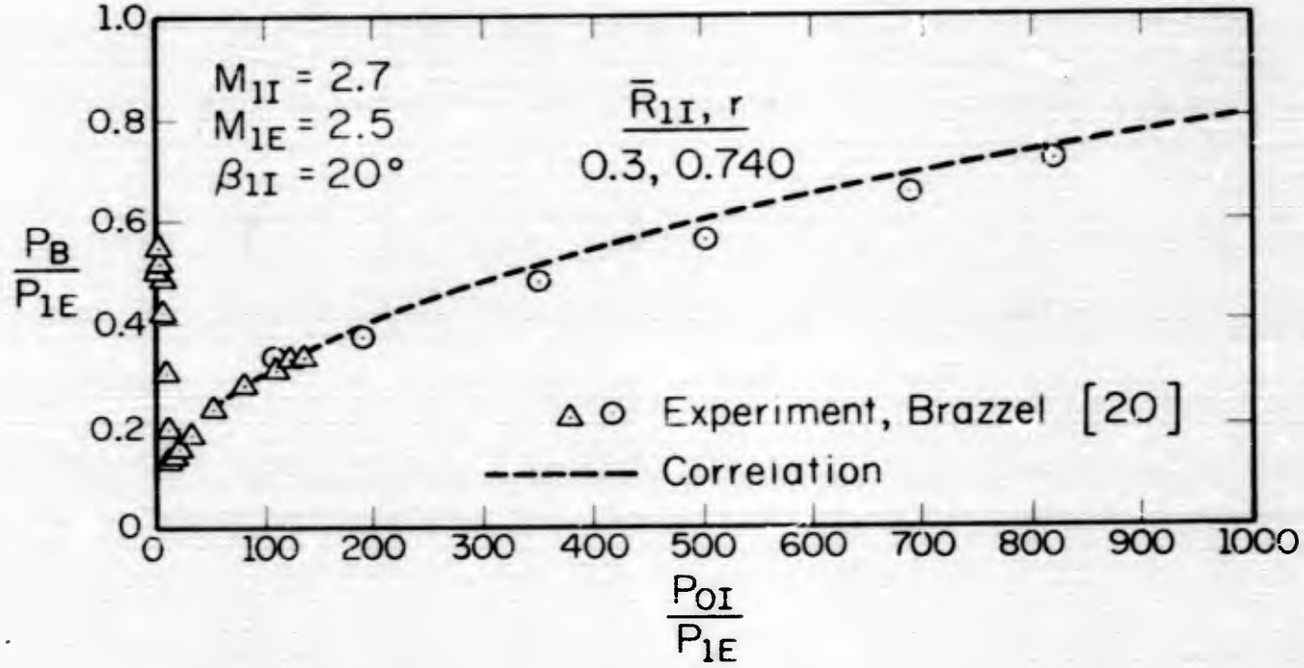

(d) Large-range Variations in P_{o1}/P_{1E} (M_{1E} = 2.5, M_{1I} = 2.7, β_{1I} = 20°)

Figure 16. continued

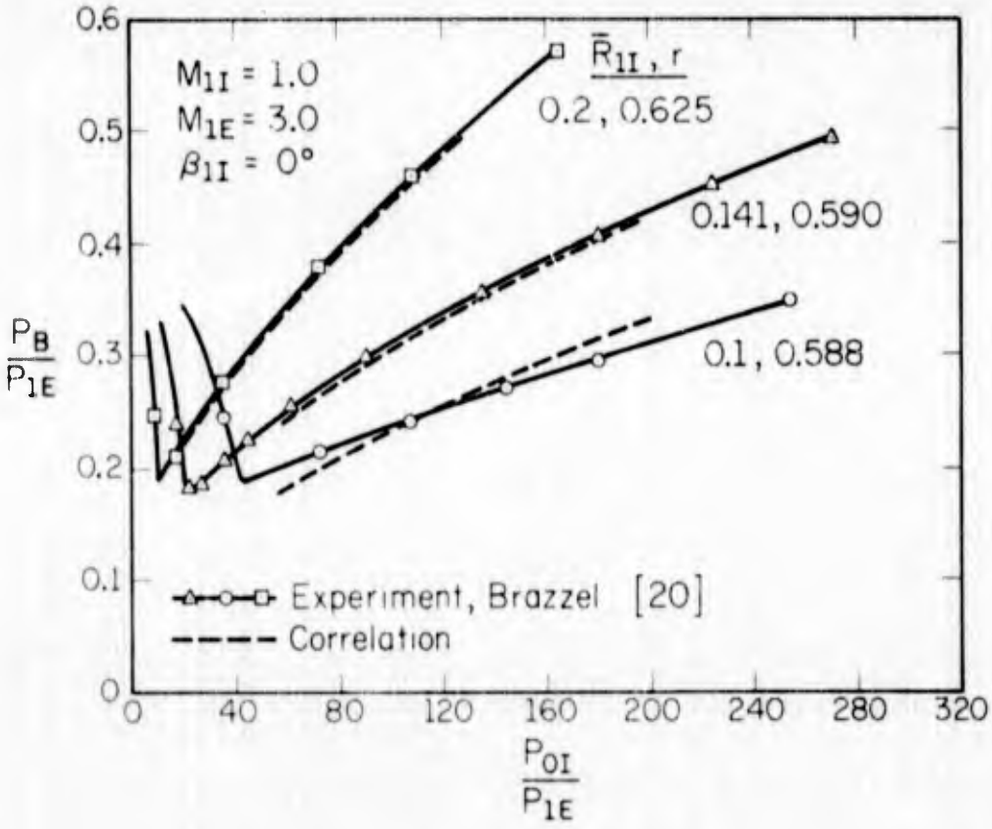

(e) Variations in $\bar{R}_{1I}$ (M_{1E} = 3.0, M_{1I} = 1.0, β_{1I} = 0°)

Figure 16. continued

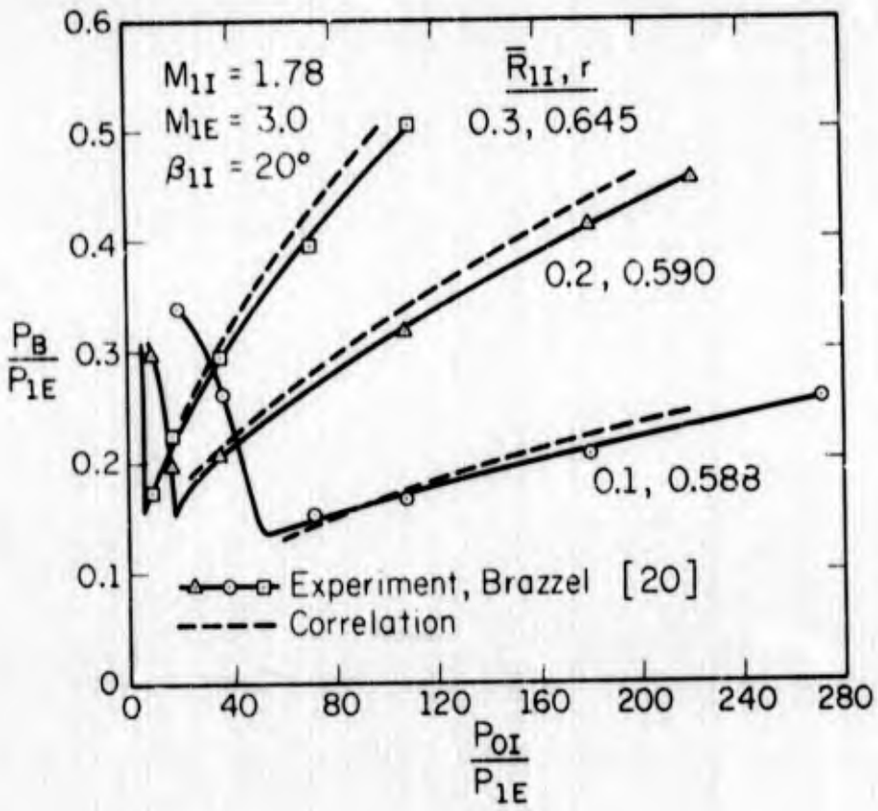

(f) Variations in $\bar{R}_{1I}$ (M_{1E} = 3.0, M_{1I} = 1.78, β_{1I} = 20°)

Figure 16. continued

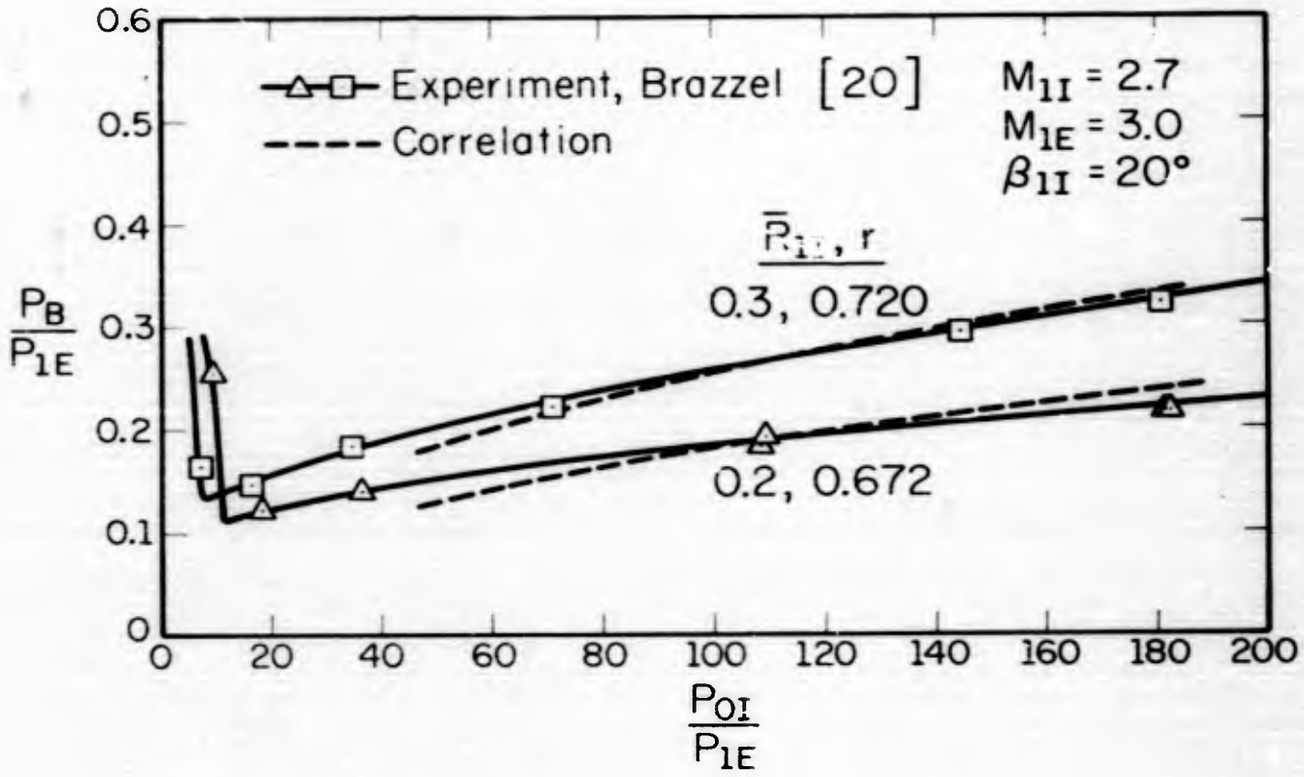

(g) Variations in $\bar{R}_{1I}$ (M_{1E} = 3.0, M_{1I} = 2.7, β_{1I} = 20°)

Figure 16. continued

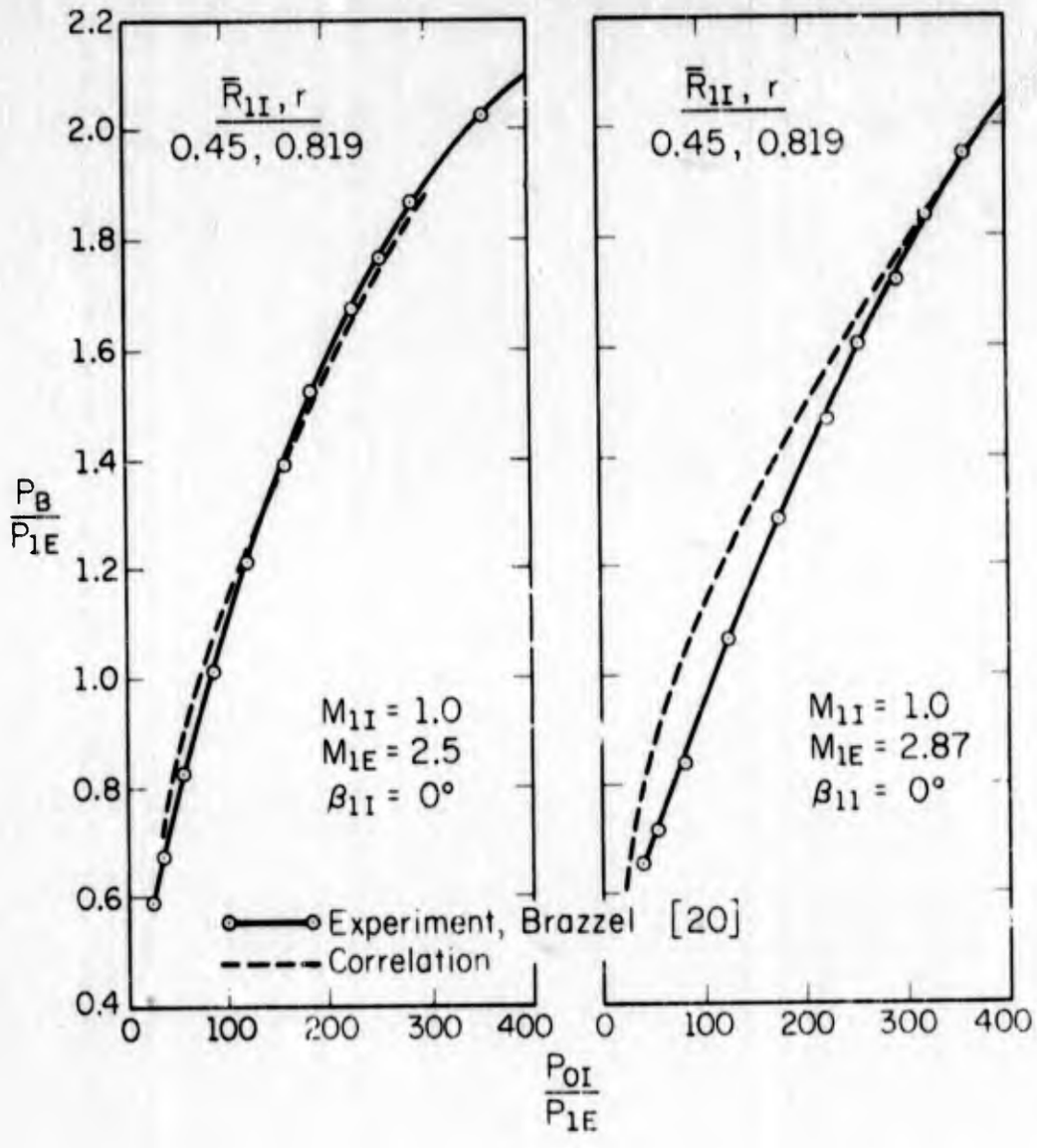

(h) Variations in M_{1E} (M_{1I} = 1.0, $\bar{R}_{1I}$ = 0.45)

Figure 16. continued

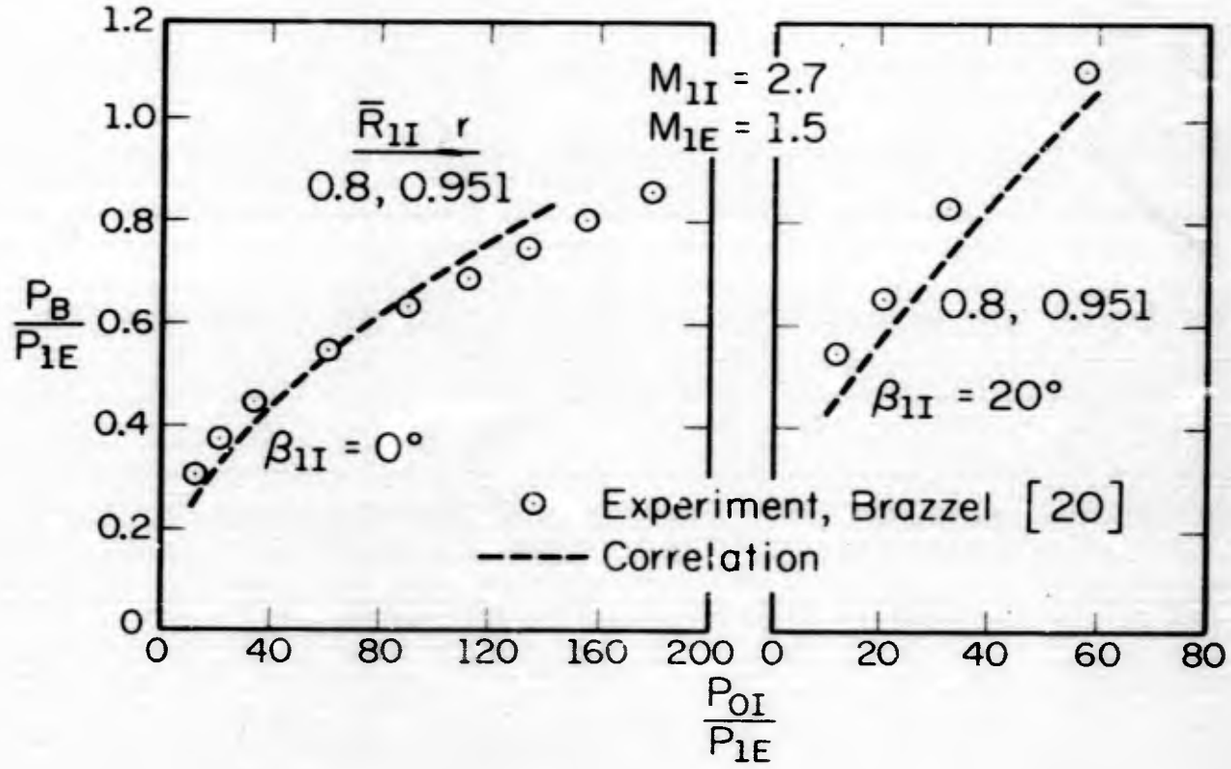

(i) Variations in β_{1I} (M_{1E} = 1.5, M_{1I} = 2.7, R_{1I} = 0.8)

Figure 16. continued

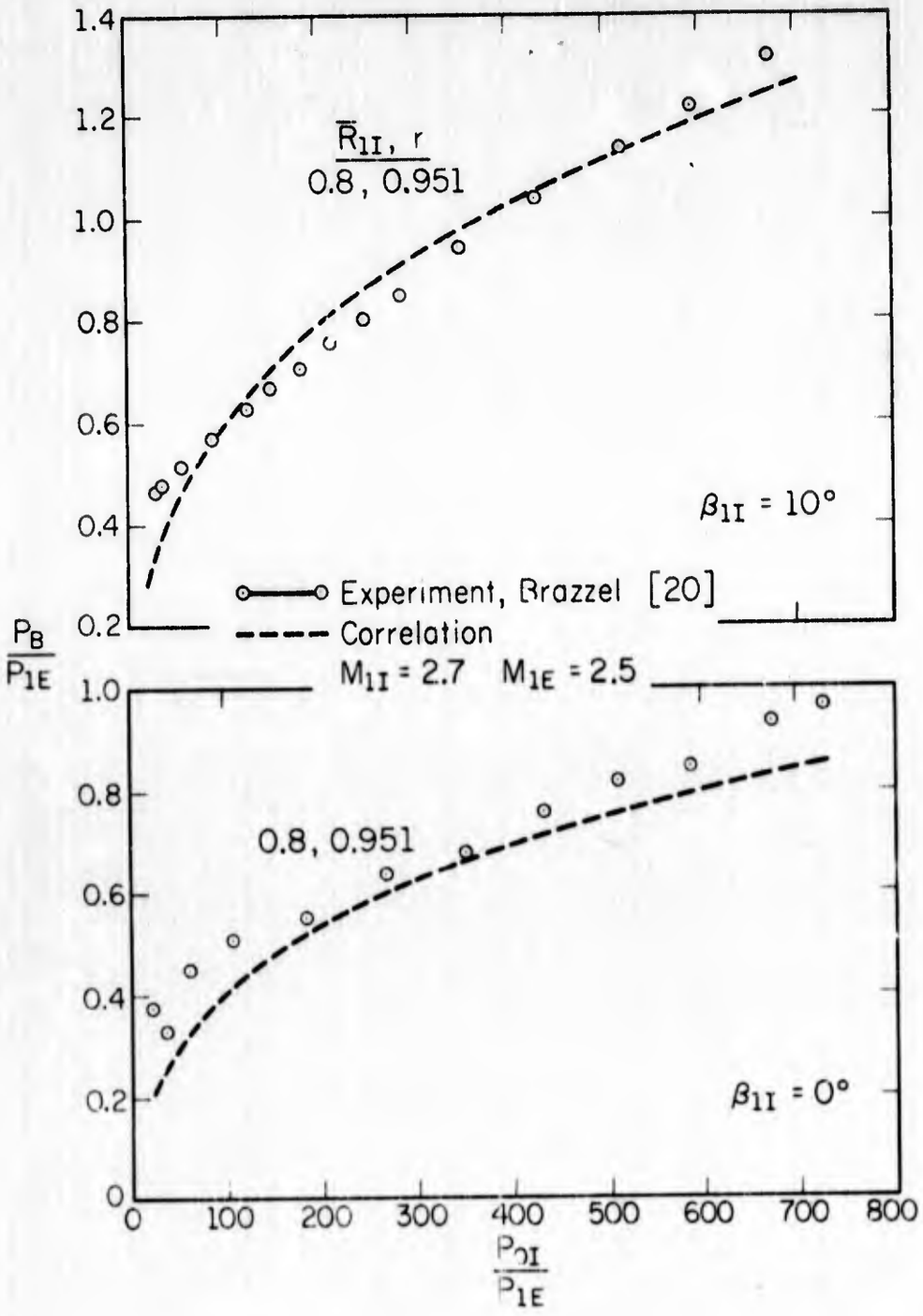

(j) Variations in β_{1I} ($M_{1E} = 2.5$, $M_{1I} = 2.7$, $R_{1I} = 0.8$)

Figure 16. continued

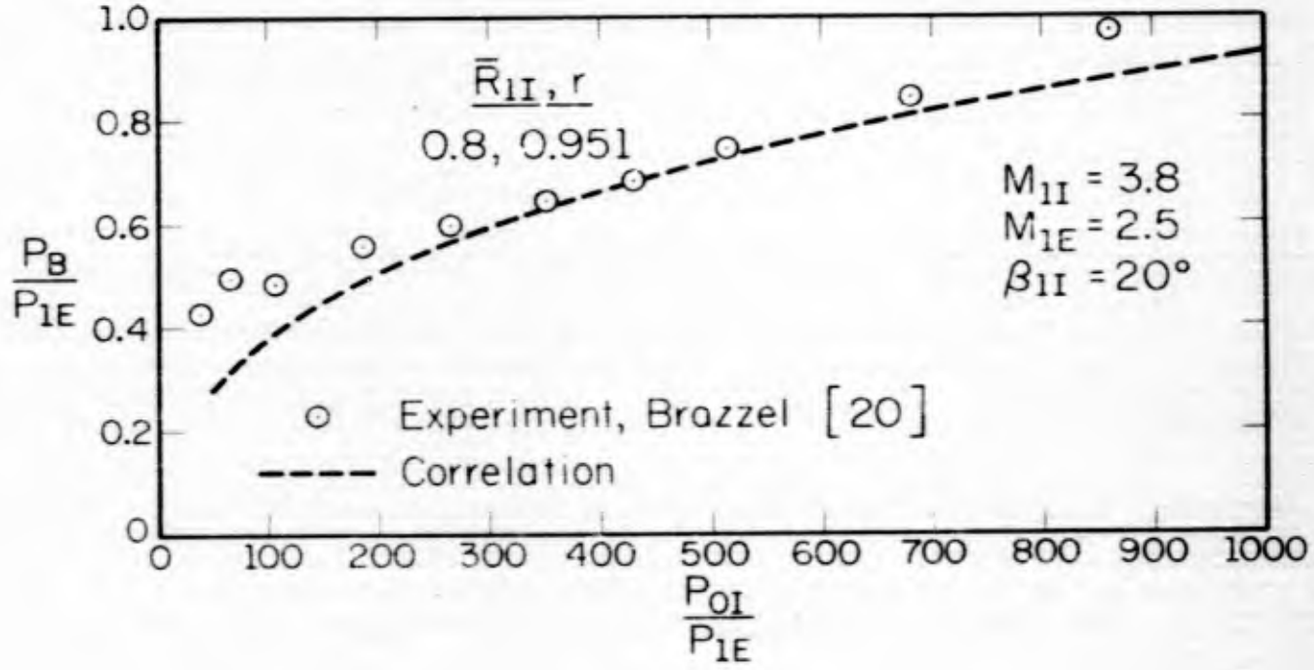

(k) Large-range Variations in P_{oI}/P_{1E} (M_{1E} = 2.5, M_{II} = 3.8, β_{II} = 20°, $\bar{R}_{II}$ = 0.8)

Figure 16. continued

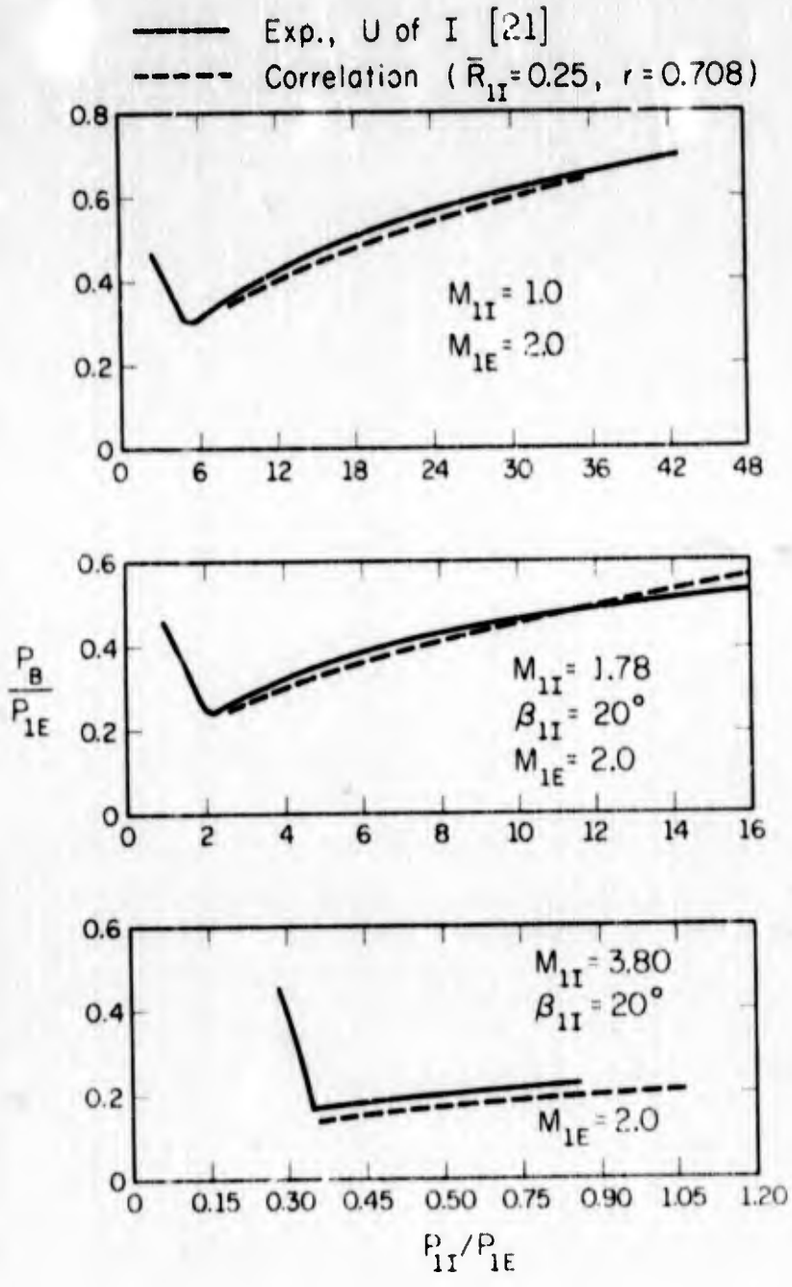

(a) Variations in M_{1I}

Figure 17. A Limited Comparison with the Data Obtained at the University of Illinois at Urbana-Champaign [21]

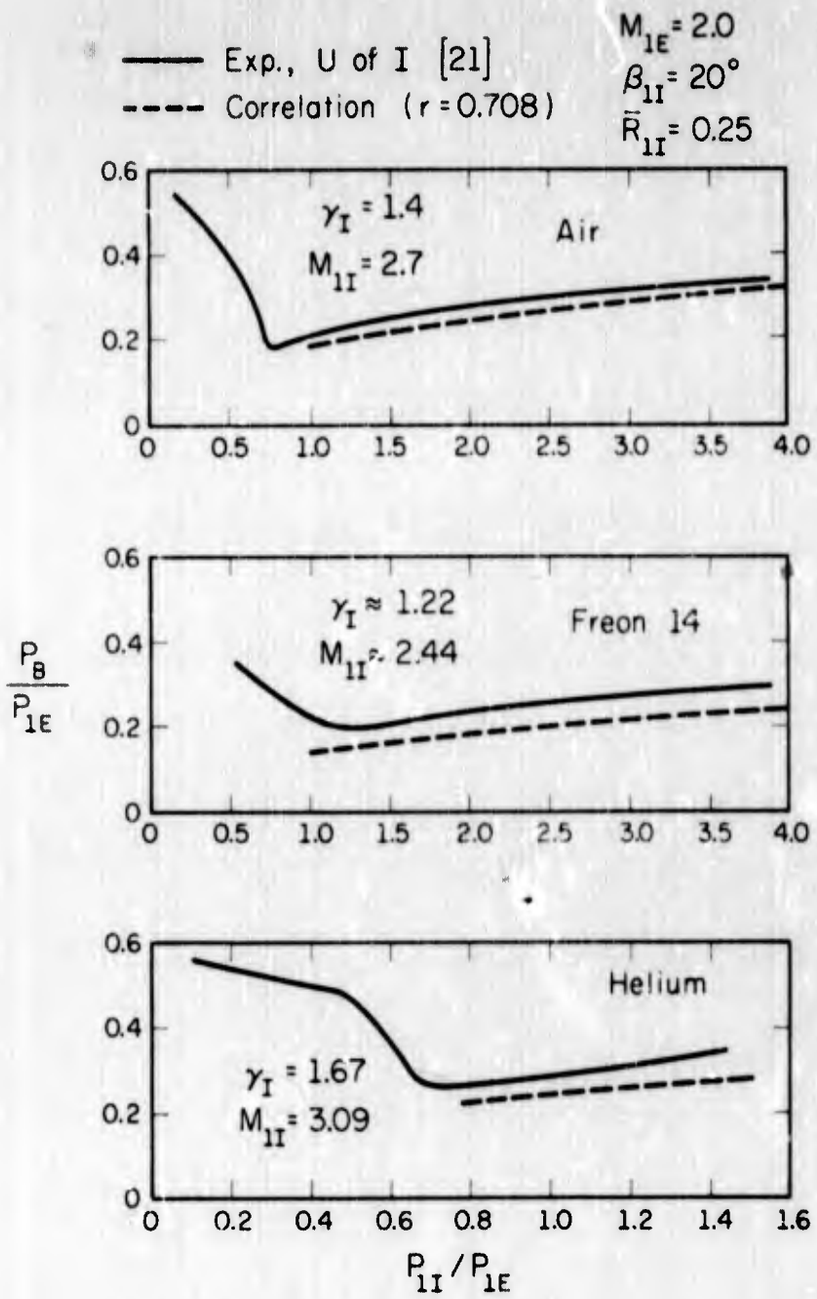

(b) Variations in γ_I

Figure 17. continued

UNCLASSIFIED

Security Classification

DOCUMENT CONTROL DATA - R & D

(Security classification of title, body of abstract and indexing annotation must be entered when the overall report is classified)

1. ORIGINATING ACTIVITY (Corporate author)
Advanced Systems Laboratory
Research and Engineering Directorate (Provisional)
U. S. Army Missile Command
Redstone Arsenal, Alabama 35809

2a. REPORT SECURITY CLASSIFICATION
Unclassified

2b. GROUP
N/A

3. REPORT TITLE
ANALYSIS OF THE AXISYMMETRIC BASE-PRESSURE AND BASE-TEMPERATURE PROBLEM WITH SUPERSONIC INTERACTING FREESTREAM-NOZZLE FLOWS BASED ON THE FLOW MODEL OF KORST, ET AL.: PART II

4. DESCRIPTIVE NOTES (Type of report and inclusive dates)
Technical Report

5. AUTHOR(S) (First name, middle initial, last name)
A. L. Addy

6. REPORT DATE	7a. TOTAL NO. OF PAGES	7b. NO. OF REFS
31 December 1969	67	21

8a. CONTRACT OR GRANT NO.	9a. ORIGINATOR'S REPORT NUMBER(S)
b. PROJECT NO. (DA) 1M62301A206	RD-TR-69-13
c. AMC Management Structure Code No. 522A.11.14800	9b. OTHER REPORT NO(S) (Any other numbers that may be assigned this report)
d.	AD

10. DISTRIBUTION STATEMENT
This document is subject to special export controls and each transmittal to foreign governments or foreign nationals may be made only with prior approval of this Command, ATTN: AMSMI-RD.

11. SUPPLEMENTARY NOTES	12. SPONSORING MILITARY ACTIVITY
None	Same as No. 1

13. ABSTRACT

The functional behavior and the effects of the many geometric and flow variables on the base-pressure and base-temperature ratios can be qualitatively predicted with the flow model of Korst, et al. Although the predicted trends are correct, the discrepancy between predicted and experimental values of the base-pressure ratios can be significant under certain conditions of geometry and flow. To improve predicted-experimental agreement and to establish a basis for a quantitative analysis of the base-pressure problem with this flow model, a modification to the flow model based on an empirically determined recompression coefficient is proposed. The recompression coefficient and its principal dependence on the nozzle-to-base radius ratio are established by detailed comparisons with experiment over a wide range of the governing variables. The recompression coefficient and the detailed comparisons with experimental data are presented herein.

DD FORM 1 NOV 68 1473 REPLACES DD FORM 1473, 1 JAN 64, WHICH IS OBSOLETE FOR ARMY USE.

UNCLASSIFIED

Security Classification

14 KEY WORDS	LINK A		LINK B		LINK C	
	ROLE	WT	ROLE	WT	ROLE	WT
Predicted flow variables Base-pressure ratios Base-temperature ratios Flow model Recompression coefficient						